

Publishers' page

Publishers' page

Publishers' page

Publishers' page

## CONTENTS

Foreword	vii
Preface	ix
Multilevel methods in Large-Eddy Simulation <i>Pierre Sagaut</i> <sup>1</sup> and <i>Marc Terracol</i> <sup>2</sup> P. Sagaut and M. Terracol <sup>3</sup>	3



## FOREWORD

foreword



## PREFACE

preface

## CONTENTS



## MULTILEVEL METHODS IN LARGE-EDDY SIMULATION

Pierre Sagaut <sup>1</sup> and Marc Terracol <sup>2</sup>

<sup>1</sup> *Laboratoire de Modélisation en Mécanique  
Université Pierre et Marie Curie, 4 place Jussieu, case 162  
75252 Paris Cedex 5, France*

*E-mail: Pierre.Sagaut@upmc.fr*

<sup>2</sup> *ONERA, CFD & Acoustics Department  
29 avenue de la Division Leclerc  
92 Châtillon cedex, France  
E-mail: terracol@onera.fr*

Issues related to the use of multilevel-based methods within the Large-eddy simulation (LES) framework are discussed. The bases of Large-eddy simulation for incompressible turbulent flows are first recalled. The emphasis is put on the mathematical models for LES and the subgrid modeling issue. In a second time, a general multiresolution/multiscale framework is introduced, which extend the usual definition of LES. Using this new tool, general features of multilevel LES methods are discussed and illustrated.

### 1. Introduction

It is well known that the unsteady simulation of turbulent flows leads to some very high numerical costs. This is due to the complexity of the turbulent phenomenon, in which a very wide range of characteristic scales are present, in both space and time. The numerical resolution of a turbulent flow thus requires the use of a very high number of degrees of freedom, since all these characteristic scales must be resolved, ranging from the largest energy-containing scales to the smallest dissipation scales (referred to as the Kolmogorov scales in the energy cascade theory). A commonly used scaling shows that the number of degrees of freedom to be used for the simulation of a turbulent flow is proportional to  $Re^3$ , where  $Re$  denotes the Reynolds number. Since practical problems are characterized by some

rather high values of the Reynolds number (typically several millions), the Direct Numerical simulation of a turbulent problem is still out of reach of the capabilities of present supercomputers. The only way to simulate such flows is then to reduce significantly the complexity of the problem, *i.e.* to reduce the number of degrees of freedom. An efficient way to do so is to perform a scale segregation. Indeed, the smallest scales of the flow are shown to exhibit a more universal behavior than the large ones, and to be associated to some much lower energy contents. The Large-Eddy Simulation (LES) technique relies on this observation, and proposes to resolve only the largest scales of the flow, while the smallest ones are only taken into account through the use of a mathematical model. However, one limitation for LES relies in the fact that the subgrid models can only account for a limited amount of (simple) flow phenomena. This yields to some prohibitive computational costs when the considered flows are governed by some coherent structures associated to a wide range of characteristic lengths and frequencies. Indeed, such flow structures may be highly anisotropic, and require a deterministic resolution, leading to the use of very fine computational meshes and small time steps.

It thus appears that the practical applicability of LES is limited by two main difficulties: the first one is due to a lack of generality of the subgrid models which are developed under some rather strong physical assumptions, and thus do not account for complex flow phenomena. The second one is due to the computational cost of the simulations which is very high, and thus limits the use of LES to low Reynolds numbers and simple configurations.

Remembering that turbulence is a multiscale phenomenon, in which each range of characteristic scales is subjected to a specific physics, it appears interesting to investigate some methods which take directly into account this specificity. Such methods, referred to as the multilevel methods, have been developed to perform some specific numerical treatments for each range of characteristic scales. The contribution of these methods to the numerical simulation of turbulent flows is double. Indeed, since the different characteristic scales are treated thanks to some adapted strategies, these methods contribute to the development of some enhanced subgrid models, resulting (at a similar cost than conventional LES) in an improvement of the global accuracy of the simulations. Another way to take advantage of such methods is to reduce the computational effort dealing with the smallest resolved scales, resulting in a significant reduction of the global cost of the simulation, at a similar degree of accuracy compared to conventional LES.

In the first part of this chapter, the basis of classical Large-Eddy Simulation will first be recalled. Focus will particularly be made on the practical interpretation of this numerical technique, and on existing subgrid closures. In the second part, the more specific context of the multiscale/multiresolution methods will be investigated. Some particular multilevel methods relying on the use of a multigrid discretization of the physical domain will be detailed and discussed.

## 2. The Large-Eddy Simulation Technique

### 2.1. Introduction to the LES Concept

The LES concept consists in directly capturing the dynamics of a targeted range of wave numbers (see [35] for an introduction). As indicated by its name, small<sup>a</sup> scales are discarded while large scales are resolved on the computational grid. Retaining only large scales makes it possible to define a solution which is smoother than the original Navier–Stokes solutions, since the gradients of the new solution will be weaker. This is why this scale separation step can also be interpreted as a regularization (some authors interested in mathematical analysis also use the term mollification - see [3] for a survey of mathematics of LES) of the Navier–Stokes solution.

This simple empirical definition of LES yields several possible interpretations, which can be found in the existing literature:

- LES is a numerical technique. This point of view is related to the fact that performing LES corresponds to solving the Navier–Stokes equations on a grid that is too coarse to allow the capture of all active scales of the exact solution. To recover a relevant solution, it is known that a source term must be added to the *discretized equations*. From a physical standpoint, this forcing term is expected to account for the influence of missing scales on the resolved ones. From a more formal point of view, the forcing term is designed to stabilize the orbit of the discrete chaotic dynamical system associated to the discrete problem.
- LES is a physical model. The set of solved equations are interpreted as a physical model for fluid turbulence at large scales. The scale separation is assumed to be carried out using a controlled mathematical operator (the most popular one being the convolution filter paradigm introduced by Leonard). The non-linear terms,

---

<sup>a</sup>the notion of small scales is to be discussed below

which are responsible for the coupling between different scales, are therefore split into a resolvable and computable part (which is to be directly evaluated during the computation from the available data) and a subfilter part. The latter relies on missing scales and therefore should be replaced by a model, referred to as the subgrid model.

What is really LES ? None of the two interpretations mentioned above appear to be really able to account for the full LES complexity. The key questions that every LES practitioner is interested in are

- (1) In a given LES computation, i.e. for a given combination of computational grid, numerical method, subgrid model (if any), boundary and initial conditions, what are the resolved and the subgrid scales ?
- (2) What are the properties of the resolved scales, and how close are they from the corresponding scales in the exact solution ? In other words, what is the physical information contained in the result of a LES simulation ?

The exact answers to these two questions remain unknown are a timely research topics. Only very few theoretical analyzes or dedicated experimental studies are devoted to these problems, while they are in fact indirectly addressed in all research works including assessment of a LES computation by comparison with DNS or experimental data. What is learned from existing researches is that the definition of the resolved scale depends on all the parameters of the simulation, including purely numerical ones.

What is also known is that reliable results for application purposes can be recovered if both the grid generation, the numerical error and source term ( physics-grounded subgrid models or mathematically derived source term) are controlled. Here, reliable means that satisfactory of them mean flowfield is recovered, along with a physically relevant description of the fluctuating motion (Reynolds stresses, turbulent kinetic energy spectrum). Two-point and two-time correlations of the largest resolved scales (i.e. scales whose characteristic length is significantly larger than the mesh size) are also commonly recovered in a satisfactory way. But the status of small resolved scales, which are the most sensitive to numerical error and source term, is less clear. The separation between these *fully physical resolved scales* and *partially corrupted resolved scales* is observed to be case-dependent.

The rest of this section is devoted to a brief survey of the main *existing mathematical models* for LES.

## 2.2. Scale separation: from practice to theory

As mentioned above, the true LES problem (i.e. what is really done on a computer) cannot be analyzed without explicit reference to the computational grid and the numerical method. This lack of generality renders the theoretical analysis very difficult, and some mathematical models for the general LES problem are very often used to get some information on the nature and the properties of the LES solution.

### 2.2.1. The filtered Navier-Stokes equations model

The most popular theoretical model for the LES problem is the system of filtered Navier-Stokes equations, as proposed by Leonard in the 1970s [26]. The underlying idea is that the main property of the LES solution is that it appears as a regularized, smoothed solution of the Navier-Stokes equations since the small scales have been erased. It is assumed here that there exists a characteristic cutoff length  $h_r$ . The gradients of the LES solution are expected to be less intense and the correlation length of the resolved fluctuations to be greater than or equal to that of the exact solution. The true, discrete LES solution  $u_h$  is then approximated by  $\bar{u}$ , which is the filtered Navier-Stokes solution defined like

$$\bar{u}(x, t) \equiv G(\Delta) \star u(x, t) = \int_{\Omega} G(\Delta, x, y) u(y, t) dy \quad (1)$$

where  $G(\Delta, x)$  and  $\Delta$  are the filter kernel and the filter characteristic length, respectively. Here,  $\Delta$  will play the role of  $h_r$  and all the properties of the numerical method are condensed in the definition of  $G$ . The filter kernel in Eq. (1) is expressed as a function of space coordinates only, since almost all explicit LES published at present time rely on the concept of spatial filtering. Common filter kernels are displayed in Table 1.

Name	$G(\Delta, x, x')$	$\hat{G}(k)$
Gaussian filter	$\sqrt{\frac{6}{\pi\Delta^2}} \exp(-\frac{6 x-x' ^2}{\Delta^2})$	$\exp(-\frac{k^2\Delta^2}{24})$
Sharp Cut-off filter	$\frac{\sin((x-x')k_c)}{((x-x')k_c)}, k_c = \frac{\pi}{\Delta}$	$\begin{cases} 1 & \text{if } k \leq k_c \\ 0 & \text{otherwise} \end{cases}$
Box/Top Hat filter	$\begin{cases} 1/\Delta & \text{if }  x-x'  \leq \frac{\Delta}{2} \\ 0 & \text{otherwise} \end{cases}$	$\frac{\sin(k\Delta/2)}{(k\Delta/2)}$

The use of the convolution filter model for LES is a convenient simplifi-

cation of the true LES problem, but it has some drawbacks and specificities which are now discussed.

The first point is that it does not account for the projection error: the filtered solution is a continuous solution involving an infinite number of degrees of freedom. It still requires to be projected onto a discrete, finite-dimension basis to fully mimic the properties of the true LES solution. In accordance with this remark and observing that no scale smaller than  $h_r$  can be captured, several authors (e.g. Carati et al. [5]) advocated that the LES approach requires a double filtering model: a first sharp cutoff filter with cutoff length  $2\Delta$  to account for the grid Nyquist cutoff and a second filter with a smoother transfer function and the same cutoff length to account for the properties of the numerical method. This twice filtered model is discussed in the next section.

The main drawback of filtered Navier-Stokes model for LES appears when the corresponding governing equations are sought. For the sake of convenience, the presentation will be done using a generic conservation law system. The full system of filtered Navier-Stokes equations for incompressible flows is presented below. The filtered equations are derived by applying the convolution filter to the original set of equations, yielding :

$$\overline{\frac{\partial u}{\partial t}} + \overline{\nabla \cdot F(u, u)} = 0 \quad (2)$$

The next step consists in restricting the possible choices for the filter kernel and retaining filters complying with the following constraints:

- (1) Uniform fields are not modified by the filtering process, leading to

$$\int_{\Omega} G(\Delta, y) dy = 1 \quad (3)$$

- (2) The filter commutes with both time and space derivatives:

$$\left[ \frac{\partial}{\partial s}, G \star \right] (u) \equiv 0, \quad s = x, t \quad (4)$$

where the commutator is defined like  $[f, g](u) = f(g(u)) - g(f(u))$ .

Using such a filter, the filtered LES model simplifies as an evolution equation for the filtered field  $\bar{u}$ :

$$\frac{\partial \bar{u}}{\partial t} + \nabla \cdot \overline{F(u, u)} = 0 \quad (5)$$

The closure problem is here formally similar to the one encountered when dealing with Reynolds-Averaged Numerical Simulations (RANS): the unknown term  $\overline{F(u, u)}$  must be expressed as a function of  $\bar{u}$ , leading to

$$\frac{\partial \bar{u}}{\partial t} + \nabla \cdot F(\bar{u}, \bar{u}) = \nabla \cdot \left( F(\bar{u}, \bar{u}) - \overline{F(u, u)} \right) = \mathcal{F}_{\text{LES}} \quad (6)$$

where  $\mathcal{F}_{\text{LES}}$  is the subgrid force. This term can not be exactly evaluated and must then be *modelled*.

The simple derivation process detailed above is based on the very stringent constraint (4), which is obviously unrealistic when bounded domains are considered (and that is of course the case in most practical LES problems !). Bounded domains imply that the support of the filter kernel (or equivalently the cutoff length) must be changed when approaching the domain boundary  $\partial\Omega$  to keep a well-posed problem. The use of a position-dependent (i.e. non-homogeneous) filter kernel automatically introduces some commutation errors, whose following compact expression was given by Fureby and Tabor [15]

$$[\nabla, G\star](u) = \nabla \Delta \left( \frac{\partial G}{\partial \Delta} \star u \right) + \int_{\partial\Omega} G(x-y, \Delta(x))u(y)dy \quad (7)$$

The first term account for the space gradient of the cutoff length while the second one arises from the trace of  $G$  on the domain boundary. It is also very important to notice that the use of non-homogeneous filters is also a way to model the effect of non-uniform grids in true LES computations. Equation (7) reveals that the set of governing equations obtained using a non-homogeneous filter kernel are much more complicated than Eq. (6), and Ghosal and Moin [17] have shown that it can even yields inconsistent equations if no additional constraint are imposed on  $G$ . This analysis was extended by Vasilyev et al. [45], who showed that the commutation error scales as  $\Delta^p$  if the moments of order 1 to  $(p-1)$  of the convolution kernel are identically zero and all higher-order moments are bounded. The main remaining problem is here to find kernels  $G$  fulfilling these conditions.

Another way to derive filtered Navier-Stokes equations which mimic the use of structured non-uniform computational grids was proposed by Jordan [21], who observed that most of the problems arise from the fact that the Navier-Stokes equations, written in Cartesian coordinates, are first filtered and then rewritten in general coordinates. Inverting these two operations, i.e. first writing the equations in general coordinates and then filtering them,

makes it possible to use constant-cutoff length filters (but the problem of the definition of  $\bar{u}$  on  $\partial\Omega$  remains). This is illustrated writing the model conservation law system in general coordinates:

$$\frac{\partial J^{-1}u}{\partial t} + \nabla_{\xi} \cdot F_{\xi}(U^{\xi}, u) = 0 \quad (8)$$

where  $J^{-1}$  is the Jacobian of the transformation, and  $\nabla_{\xi}, F_{\xi}$  and  $U^{\xi}$  are the gradient in the reference space, the flux in the reference space and the contravariant unknowns, respectively. The new coordinate system being associated with a uniform grid distribution, an homogeneous filter is used, ensuring that the filtering operator now commutes with the space derivatives, yielding

$$\frac{\partial \overline{J^{-1}u}}{\partial t} + \nabla_{\xi} \cdot F_{\xi}(\overline{U^{\xi}}, \bar{u}) = \nabla_{\xi} \cdot \left( F_{\xi}(\overline{U^{\xi}}, \bar{u}) - \overline{F_{\xi}(U^{\xi}, u)} \right) \quad (9)$$

The difficulty is now that the subgrid terms appearing in the right-hand side of Eq. (9) involves metric terms and contravariant quantities, whose behavior can not be directly analyzed on the grounds of the dynamics of turbulent flows. This problem can be partly simplified assuming that the geometric parameters are invariants of the filtering operation, since they are computed using discrete schemes and can be considered as being already filtered. Explicit model derivation is more complicated than in the previous case, since unknowns cannot be directly tied to physical quantities (contravariant velocity cannot be measured in a wind tunnel!) As a consequence, functional models used within this framework are most of the times obtained by translating the usual models derived in the previous approach which rely on physical unknowns.

### 2.2.2. *A more realistic model: the twice-filtered Navier-Stokes equations*

The filtered Navier-Stokes equations model discussed above can not account for all the error sources present in the true LES problem when simple filter kernels are considered (see Table 1). To recover a more realistic mathematical model still based on the convolution filter approach, several authors use a double-filtering technique:

- A first filter (usually a smooth filter such as the Gaussian filter or the box filter) which will account for the smoothing properties of the

LES approach. It is exactly the same filtering step as in the preceding section. The cutoff length is usually related to the resolution length  $h_r$ , and thus accounts for some features of the numerical method used in the true LES problem. The scales removed by this filter are referred to as the *subfilter scales*. The associated field convolution is written as  $\bar{u} = \bar{G} \star u$ .

- A second filter, which is a spectral sharp cutoff filter related to the Nyquist cutoff frequency of the computational grid,  $h$ . The scales filtered out at this stage are called the *subgrid scales*. This filter level is noted as  $\tilde{u} = \tilde{G} \star \bar{u} = \tilde{G} \star \bar{G} \star u$ .

The introduction of that new second filtering step aims at taking into account the fact that scales of motion smaller than the Nyquist cutoff length are irremediably lost in the true LES problem. The use of a single smooth filter does not permit to account for this loss of information since smooth filters can be inverted, allowing a theoretical perfect reconstruction of the exact solution. The special case of the single filter approach based on the sharp cutoff filter is also consistent with the true LES problem, but it represents only the special case of LES computations carried out using Fourier spectral methods.

Within the double-filter approach, the true LES solution is approximated as  $\tilde{u}$  (where the bar and tilde symbols are related to the first and second filtering step, respectively), which is solution of

$$\frac{\partial \tilde{u}}{\partial t} + \nabla \cdot F(\tilde{u}, \tilde{u}) = \nabla \cdot \left( F(\tilde{u}, \tilde{u}) - \widetilde{F(u, u)} \right) \quad (10)$$

The unknown term in the right hand side can be further decomposed introducing the triple decomposition

$$u = \tilde{u} + u' + u'' \quad (11)$$

where

- $\tilde{u}$  represents the scales that are captured on the grid and resolved in the sense that they are not destroyed by the smooth filter
- $u'$  are the subfilter scales which are captured on the computational grid: these scales are not part of the approximate LES solution, but could be computed on the computational grid
- $u''$  are the "true" subgrid scales, i.e. the scales which can not be computed on the grid and are definitively missing.

The field that can be captured on the grid is thus equal to  $\tilde{u} = \tilde{\tilde{u}} + u'$ . According to this decomposition, one obtains

$$\begin{aligned} \overline{F(u, u)} &= \underbrace{\overline{F(\tilde{\tilde{u}}, \tilde{\tilde{u}})}}_{F_0} + \underbrace{\overline{F(u', \tilde{\tilde{u}})} + \overline{F(\tilde{\tilde{u}}, u')} + \overline{F(u', u')}}_{F_1} \\ &\quad + \underbrace{\overline{F(\tilde{\tilde{u}} + u', u'')}}_{F_2} + \underbrace{\overline{F(u'', \tilde{\tilde{u}} + u')}}_{F_3} + \underbrace{\overline{F(u'', u'')}}_{F_3} \end{aligned} \quad (12)$$

The two first terms,  $F_0$  and  $F_1$ , involve only scales than can be captured on the computational grid, and might be exactly computed if  $u'$  was known. The other terms include  $u''$  and must be modelled.

### 2.2.3. Additional mathematical models

The filtering approach is the most popular mathematical model of LES, but it was shown in the preceding section that it introduces some new problems (the main one being its extension to non-uniform grids on bounded domains) which are a priori not raised in the true LES problem. To preclude these *artefacts* of the filtering approach, a few authors recommend using statistical operators or projection operators rather than a convolution filter.

A procedure based on conditional elimination of the small scales was advocated independently by McComb [30] and Yoshizawa [48]. The underlying idea is that the random chaotic character of the turbulent motion is more pronounced at the very small scales than at the larger one. The rationale behind this hypothesis, referred to as the *local chaos hypothesis* (localness being in terms of wave number) is close to the Kolmogorov's local isotropy assumption: very small scales are isotropic and decorrelated from the large ones, which are deterministically affected by the boundary conditions, and therefore are more uncertain than the latter. That loss of memory is consistently associated with the picture of the kinetic energy cascade. The associated scale separation procedure is a statistical average over scales smaller than  $\Delta$ , larger scales being left unchanged.

The main advantage of this procedure is that the artefacts of the convolution filter are now avoided, but, since it rely on a statistical average, several realizations of the flow are required, while the convolution filter procedure requires only one. This requirement is not important from a purely theoretical viewpoint, but it makes the statistical procedure very difficult to implement in practice.

The use of a projection operator to model the LES problem was advocated by several authors, the most popular approach being the Variational Multiscale Method developed by Hughes and coworkers [19, 20]. Writing the full solution as the sum of orthogonal components (or, in an equivalent way, decomposing the solution space as a sum of orthogonal subspaces):

$$u \in \mathcal{W}, \quad \mathcal{W} = \mathcal{W}_1 \oplus \mathcal{W}_2 \oplus \dots \quad (13)$$

an elegant model for the LES problem is obtained by truncating the sum and discarding some components (i.e. operating a projection onto an arbitrary subspace  $\mathcal{W}_h$  spanned by an arbitrary set of  $\mathcal{W}_i$ , yielding

$$u_h \in \mathcal{W}_h, \quad u' \equiv (u - u_h) \in \mathcal{W}' = \mathcal{W} - \mathcal{W}_h \quad (14)$$

This approach is a natural one to analyze the properties of LES simulations relying on variational numerical methods such as finite elements.

### 2.3. Usual Navier–Stokes-based equations for LES

The filtered Navier–Stokes equations, assumed to be a reliable mathematical model for LES, are given in this section. The convolution filter is supposed to commute with all space and time derivatives.

The filtered Navier–Stokes equations for an incompressible flow read:

$$\frac{\partial \bar{u}}{\partial t} + \nabla \cdot (\overline{u \otimes u}) = -\nabla \bar{p} + \nu \nabla^2 \bar{u} \quad (15)$$

$$\nabla \cdot \bar{u} = 0 \quad (16)$$

The non-linear term  $\overline{u \otimes u}$  must be decomposed as a function of the acceptable unknowns, namely  $\bar{u}$  and  $u'$ .

The following decomposition was proposed by Leonard (Leonard, 1974). It is obtained by inserting the decomposition  $u = \bar{u} + u'$  into the non-linear term, yielding:

$$\overline{u \otimes u} = \overline{(\bar{u} + u') \otimes (\bar{u} + u')} \quad (17)$$

$$= \underbrace{\overline{\bar{u} \otimes \bar{u}}}_{\text{resolved}} + \underbrace{\overline{\bar{u} \otimes u' + u' \otimes \bar{u}}}_{C:\text{Cross terms}} + \underbrace{\overline{u' \otimes u'}}_{R:\text{Reynolds stresses}} \quad (18)$$

The resolved term can be expressed as:

$$\overline{\bar{u} \otimes \bar{u}} = \underbrace{\bar{u} \otimes \bar{u}}_{\text{new resolved}} + \underbrace{(\overline{\bar{u} \otimes \bar{u}} - \bar{u} \otimes \bar{u})}_{L: \text{Leonard stress tensor}} \quad (19)$$

making three tensors appearing:

- The *Leonard tensor*  $L$ , which corresponds to the fluctuations of the interactions between resolved scales (zero for RANS).
- The *Cross stress tensor*  $C$ , which accounts for direct interactions between resolved and unresolved scales (zero for RANS).
- The *subgrid Reynolds stress tensor*  $R$ , which is associated to the action of subgrid scales on the resolved field (Reynolds tensor for RANS).

Two possibilities arise for the definition of the subgrid scale tensor  $\tau$ , which depend on the choice of the formulation of the resolved convection term. The first one is

$$\tau = C + R \quad (20)$$

and corresponds to a resolved nonlinear term of the form  $\overline{\bar{u} \otimes \bar{u}}$ , while the second one is

$$\tau = L + C + R \quad (21)$$

with a resolved convection term of the form  $\bar{u} \otimes \bar{u}$ .

These two decompositions can be used, but they introduce some interesting conceptual problems. Consider the philosophy of LES: filtered equations are derived, and all the terms appearing in the equations must be filtered terms (*i.e.* appear as the filtered part of something). Only the first decomposition satisfies that condition. This is especially true when the filtering operator is associated to the definition of a computational grid (and *bar* just means "defined on the grid"): the convection term is computed on the same grid as the filtered variables, and then should be written as  $\overline{\bar{u} \otimes \bar{u}}$ . Another point is that in the first decomposition the neither the subgrid tensor nor the resolved convection term are invariant under Galilean transformations (but their sum is invariant), while in the second decomposition both terms are invariants. A more accurate analysis reveals that  $R$  and  $L + C$  are invariant for this class of transformation.

## 2.4. Brief introduction to closure strategies

Explicit LES approaches are based on the introduction of a forcing term in the governing equations ( $\mathcal{F}_{\text{LES}}$  in Eq. (8)), which can not be directly computed and must be modelled as a function of the available unknowns. As mentioned above, two classes of models can be distinguished, which are discussed below. The present survey will be restricted to models developed for Newtonian, non-reactive, single-phase flows without external forcing or multiphysics coupling such as in magnetohydrodynamics. Therefore, governing equations presented above will be used as relevant models to describe the LES problem and to present the models. It is here important to emphasize that almost all existing explicit subgrid scale models have been developed within the framework of the filtered Navier-Stokes equations.

### 2.4.1. Functional subgrid scale models

**The basic model** Functional subgrid scale models are designed to reproduce the effects of the small unresolved scales on the resolved ones. They are built on physical considerations on the nature of this interaction, and do not aim at producing a good approximation of neither the subgrid scales nor the subgrid scale tensor.

An examination of the existing literature shows that almost all functional models have been built to enforce the correct resolved kinetic energy balance. The very reason for that is that they are designed to mimic the kinetic energy cascade from large to small scales, which is known to be a universal and dominant physical mechanism in fully developed turbulent flows. More complex dynamical effects exhibit less generality and are much more difficult to take into account via a model, and are usually neglected in the functional modelling approach. Nevertheless, some modified functional models for stratified flows have been proposed (see [35] for a review). It is also worthy noticing that some effects on turbulence, such as rotation effects, are very difficult to take into account in a physical model. An important consequence is that all scales at which important physical mechanisms other than the energy cascade are at play must be directly captured during the computation to get reliable results. This results in a *physical guide* for the definition of resolved/subgrid scales in explicit LES with functional subgrid scale models.

The main effect of the kinetic energy cascade is a gross drain of the energy of the large scales (i.e. resolved scales in the present LES framework) by the small ones (i.e. subgrid scales). This drain is expressed within the

filtered Navier-Stokes framework as

$$\varepsilon_t = -\tau : \nabla \bar{u} \quad (22)$$

where  $\varepsilon_t$  and  $\tau$  are the kinetic energy cascade rate and the subgrid tensor, respectively. A simple empirical mathematical model for that is the definition of a *subgrid viscosity*  $\nu_t$  whose amplitude will be calibrated to enforce the desired mean energy loss. The resulting term in the filtered Navier-Stokes equations (in the incompressible case) is

$$\mathcal{F}_{\text{LES}} = \nabla \cdot (-2\nu_t \bar{S}), \quad \bar{S} \equiv \frac{1}{2} (\nabla \bar{u} + \nabla^t \bar{u}) \quad (23)$$

This simple approach is sustained considering the analogy with the kinetic gas theory, in which the macroscopic viscosity and diffusivity of a gas originate in the small-scale molecular motion. But it is worth noting that this is nothing but an analogy: viscosity and diffusivity characterize the fluid and can be considered as constants because there is a clear scale separation between the molecular motion and the velocity fluctuations at the macroscopic level, while there is no spectral gap in the turbulent spectrum, resulting in a flow-dependent definition of the subgrid viscosity. The idea of representing the small turbulent scale effects through the definition of a turbulent viscosity (a subgrid viscosity in the present parlance) is not new. The idea of parameterizing small scales of turbulence through the use of an effective viscosity can be traced back in the early 19th century: Saint-Venant in 1834 clearly distinguished two scales of motion in a turbulent flow, namely a larger scale at which the average (over fluid element) velocity varied smoothly in space and time, and a smaller scale at which the motion could be very irregular. In his description, the effective viscosity parameter defined at larger scales depended on the irregular motion at the small scales. Thus it could vary from one point to another and from one kind of flow to another. A consequence<sup>b</sup> of Eq. (23) is the following approximation for the subgrid tensor  $\tau$

$$\tau = -2\nu_t \bar{S} \quad (24)$$

<sup>b</sup>It is important to remark that this parametrization of the subgrid tensor is deduced from the subgrid viscosity assumption, since the functional modelling strategy does not aim at reproducing it at all.

In the incompressible flow case the tensor  $\overline{\mathcal{S}}$  is trace-free and relationship (24) holds for the deviatoric part of  $\tau$  only:

$$\tau - \frac{\tau_{kk}}{3}I = -2\nu_t\overline{\mathcal{S}} \quad (25)$$

The most popular subgrid scale viscosity model (and the oldest one in the history of modern LES) was published by Smagorinsky [39]. Remarking that the dimension of  $\nu_t$  is  $\nu_t = [L]^2[T]^{-1}$ , the problem is to identify the characteristic space- and time-scales for the subgrid-scale motion. The space scale is defined as  $C_S\Delta$  (where  $C_S$  is a constant to be adjusted to tune the model) and the time-scale is evaluated using an evaluation of the local shear  $|\overline{\mathcal{S}}| \equiv \sqrt{2\overline{\mathcal{S}} : \overline{\mathcal{S}}}$ , yielding

$$\nu_t = (C_S\Delta)^2|\overline{\mathcal{S}}| \quad (26)$$

The constant  $C_S$  can be evaluated in the very simple case of isotropic incompressible turbulence at very high Reynolds number: assuming that (i) the Kolmogorov spectrum shape  $E(k) = C_K\varepsilon^{2/3}k^{-5/3}$  (with  $C_K = 1.4$ ,  $\varepsilon$  and  $k$  the Kolmogorov constant, the turbulent dissipation rate and the wave number, respectively) is observed at all scales, and (ii) that turbulent scales are in local equilibrium (turbulent kinetic energy production rate, kinetic energy cascade rate and viscous dissipation rate are equal), the value  $C_S = 0.18$  is found and yield good LES results for that flow. But numerical experiments prove that this model is too dissipative in shear flows. This can be easily explained writing the associated subgrid scale dissipation  $\varepsilon_t$  (which appears as a sink term in the resolved kinetic energy equation and a source term in the subgrid kinetic energy equation):

$$\varepsilon_t \equiv -\tau : \overline{\mathcal{S}} = 2\nu_t\overline{\mathcal{S}} : \overline{\mathcal{S}} = (C_S\Delta)^2|\overline{\mathcal{S}}|^3 \quad (27)$$

Since the Smagorinsky model is based on the local isotropy hypothesis, its use for shear flow simulation will result in an overestimation of  $|\overline{\mathcal{S}}|$  since the mean shear will be accounted for in the evaluation of  $\overline{\mathcal{S}}$  while it should not be. That flaw is directly tied to the Gabor-Heisenberg uncertainty principle: the Smagorinsky model is local in space (it is computed using a local evaluation of the gradient) and non-local in wavenumber (all resolved scales contribute to the evaluation of  $\overline{\mathcal{S}}$ ). A direct consequence is that the Smagorinsky model (or similar subgrid-viscosity models based on

the first-order derivatives of the resolved velocity field such as the structure function model [27] or the WALE model [33]) are not consistent from the spectral point of view, i.e. they will not automatically vanish when all the scales are resolved. The limiting DNS case will not be recovered in the proper way. A good example is that Smagorinsky subgrid viscosity does not return a null subgrid viscosity when applied to a laminar Poiseuille or Couette flow (where there is no subgrid scale at all!). Since the subgrid viscosity depends directly upon the cutoff length  $\Delta$ , tuning this length makes it possible to improve the results. This is what is done in the very near wall region, where the subgrid viscosity is supposed to scale as the cube of the distance to the wall. In this region, a new definition of  $\Delta$  is employed to enforce the correct asymptotic behavior. A classical example is the van Driest damping function, which is based on the following modification of the characteristic length  $\Delta$  in the near wall region:

$$\Delta \leftarrow \Delta f_w(z), \quad f_w(z) = 1 - e^{-zu_w/25\nu} \quad (28)$$

where  $z$ ,  $u_w$  and  $\nu$  are the distance to the wall, the friction velocity and the molecular viscosity, respectively.

In high Reynolds number turbulent shear flows, a heuristic criterion to obtain satisfactory results is to choose the cutoff length  $\Delta$  such that [1]

$$\frac{L_{\varepsilon_t}}{\Delta} = 10 - 20, \quad L_{\varepsilon_t} \propto \sqrt{\varepsilon/|S|^3} \quad (29)$$

where  $\varepsilon_t$  is the turbulent dissipation and  $S$  the mean shear.

All recent improvements of the Smagorinsky model (or similar subgrid-viscosity models based on the first-order derivatives of the resolved velocity field) share the same key idea of increasing the localness of the subgrid viscosity in terms of wave number and to evaluate the subgrid term using the smallest resolved scales only. The expected benefit is twofold: first, the resulting model is expected to be self-adaptive in that sense that it will automatically vanish when all scales are resolved (i.e. when the energy of the smallest scales captured on the computational grid is zero or nearly zero) and second, the rate of energy transfer is expected to be much better predicted since the physical analysis reveals that the energy transfer is local in wavenumber<sup>c</sup>. Being more local in wave number, these improved models are less local in space and the width of their discrete stencil is larger,

<sup>c</sup>at least 75% of the energy transfer of mode  $k$  is done with modes in the range  $[k/2, 2k]$ .

yielding possible non-trivial problems dealing with their definition near the boundaries of the computational domain.

**A few improvement strategies** The main strategies for improving the basic subgrid viscosity models are now surveyed:

- (1) **Removal of the mean flow contribution.** The key idea here is to split the instantaneous resolved field  $\bar{u}(x, t)$  as the sum of its statistical mean value  $\langle \bar{u} \rangle(x, t)$  and its statistical fluctuation,  $\bar{u}''(x, t)$ . The subgrid viscosity is then evaluated using  $\bar{u}''(x, t)$ , resulting in a cancellation of the influence of the mean shear. This technique, first proposed by Schumann [37], was proved to yield good results. The main underlying problem consists in computing  $\langle \bar{u} \rangle(x, t)$ . In his original work, Schumann proposed to compute it by averaging the resolved field in directions of spatial periodicity (resulting in a fully non-local model in these directions), while Carati et al. [4] recently proposed to use several statistically equivalent simulations (performed on a parallel computer) to carry out the statistical average.
- (2) **Use of the kinetic energy at the cutoff or the subgrid kinetic energy.** The basic idea here is that the kinetic energy of the smallest resolved scales and the subgrid kinetic energy are very relevant parameters for subgrid scale detection and parametrization. The subgrid viscosity is then rewritten as

$$\nu_t = C\sqrt{q}\Delta \quad (30)$$

where  $C \simeq 0.1$  and  $q$  are a constant and the kinetic energy under consideration, respectively. In the case where the smallest resolved scale energy is looked at,  $q$  is computed applying a discrete low-pass filter, referred to as the test filter, to the instantaneous resolved field and computing the kinetic energy of the small scales deduced this way. The localness of the resulting subgrid viscosity is then directly governed by those of the test filter, and equivalently by its stencil width. This approach was first proposed by Bardina [2]. A common example is the following one-dimensional discrete test filter (where  $i$  is the grid point index and  $\phi$  a dummy variable)

$$\bar{\phi}_i = \frac{1}{4}(\phi_{i+1} + 2\phi_i + \phi_{i-1}) \quad (31)$$

The kinetic energy of the subgrid scales cannot be accurately extracted

this way, and an additional evolution equation is solved to compute it. The most common closed equation is very similar to the Kolmogorov-Prandtl model:

$$\frac{\partial q}{\partial t} + \bar{u} \nabla q = 2\nu_t \bar{S} : \bar{S} - \frac{q^{3/2}}{\Delta} + \nabla \cdot (\nu_t \nabla q) + \nu \nabla^2 q \quad (32)$$

where terms appearing on the right hand side are the production by the resolved scales, the turbulent dissipation, the turbulent diffusion and the viscous dissipation, respectively. The localness in space of the original model is not modified strictly speaking since only local quantities are used, but the equation for  $q$  introduce a non-local history effect which is equivalent. Some algebraic estimates for the subgrid kinetic energy have been proposed by several authors, which were observed to be accurate in isotropic turbulence [22].

More complex forms of the subgrid viscosity can be defined using non-linear combinations of (26) and (30), yielding the one-parameter Mixed Scale model family proposed by Sagaut and Loc [35]:

$$\nu_t = C |\bar{S}|^\alpha q^{\frac{1-\alpha}{2}} \Delta^{1+\alpha} \quad (33)$$

where  $C$  and  $\alpha$  are two real parameters.

These models yield better results than rough subgrid viscosity models, but their efficiency is very sensitive to the test filter or the way complex mechanisms such as transition are taken into account in Eq. (32).

(3) **Best constant value in the least-square sense: dynamic models.**

The idea, proposed by Germano et al. [16, 28], is to find the optimal value (local in space and time) of the constant  $C$ , i.e. the value of the constant which will minimize a given error estimate for the considered formulation of the subgrid viscosity model under consideration :  $\nu_t = Cf(\bar{u}, \Delta)$ . The localness in wave number is increased using an ad hoc error estimate based on the following exact relationship, referred to as the Germano relationship, that ties the subgrid tensor at two different filtering levels (the first one being related to the bar symbol and the second - the test filter with cutoff length  $\beta\Delta$ ,  $\beta > 1$  - to the bar symbol):

$$\underbrace{(\widehat{\bar{u} \otimes \bar{u}} - \widehat{\bar{u}} \otimes \widehat{\bar{u}})}_{\mathcal{L}} - \underbrace{(\widehat{u \otimes u} - \widehat{u} \otimes \widehat{u})}_T + \underbrace{(\widehat{u \otimes u} - \bar{u} \otimes \bar{u})}_{\hat{\tau}} = 0 \quad (34)$$

where  $\tau$ ,  $T$  and  $\hat{\tau}$  are the subgrid tensor at the first filter level, the subgrid tensor at the second filter level, and the subgrid tensor at the first filter level filtered at the second level, respectively. It is important to notice that the tensor  $\mathcal{L}$  can be directly computed from the resolved LES field  $\bar{u}$  using the test filter. The next step consists in defining an error estimate. This is achieved replacing the exact subgrid tensors  $\tau$  and  $T$  by the corresponding models

$$\tau = -2Cf(\bar{u}, \Delta), \quad T = -2Cf(\hat{u}, \beta\Delta)$$

in Eq. (34), yielding the definition of the tensorial error estimate  $E$

$$E = \mathcal{L} + 2Cf(\hat{u}, \beta\Delta) - 2C\widehat{f(\bar{u}, \Delta)} \quad (35)$$

Assuming that the constant  $C$  is nearly constant over intervals of length  $\beta\Delta$ , one obtains the simplified formula

$$E = \mathcal{L} + 2C(f(\hat{u}, \beta\Delta) - \widehat{f(\bar{u}, \Delta)}) = \mathcal{L} + 2CM \quad (36)$$

To get a scalar subgrid viscosity Lilly [28] propose to compute  $C$  to minimize  $E$  in the least-square sense, leading to

$$C = \frac{1}{2} \frac{\mathcal{L} : M}{M : M} \quad (37)$$

This method is known to yield the expected properties: the subgrid viscosity vanishes in fully resolved regions and also exhibits correct asymptotic behavior in the near wall region on fine grids. It successfully decreases the dissipation of the Smagorinsky viscosity during the transition to turbulence, allowing an accurate description of the transition phase. But it has some severe drawbacks dealing with numerical stability: the constant  $C$  defined as in Eq. (37) is observed to take very large values (corresponding to mathematically ill-posed problems) and negatives values can occur over long times (leading to an exponential growth of perturbations). To cure these problems, many techniques have been proposed (see [35] for a review): to clip the constant between 0 and an arbitrary upper bound, to perform averages over homogeneous directions, closest neighbors or streamlines, or combinations of these methods. Iterative methods have also been proposed. The resulting subgrid viscosity is obviously less local in space than the original one.

Additional difficulties are known to arise when the two cutoffs (primary LES filter and test filter ones) are not located within the inertial range of the spectrum, and the procedure must be modified to recover consistent evaluations of the subgrid viscosities.

- (4) **Filtered models, Variational Multiscale Methods and hyper-viscosities.** This strategy is very close to the one based on the removal of the mean flow contribution described above, the main difference being that a low-pass filter in space is used instead of a statistical average, rendering its use more flexible. Several implementations of the same basic idea have been proposed independently, which will be described below using the framework developed by Hugues [19]. The instantaneous resolved velocity field is split into a large scale component,  $u^<(x, t)$  and a small scale component  $u^>(x, t)$ . The key idea underlying all these models consists in using  $\bar{u}$  or  $u^>$  to evaluate each term appearing in the model for the full subgrid tensor, namely the subgrid viscosity and the shear stress tensor. In practice, this splitting is achieved at each time step of the LES computation by applying a discrete test filter  $G_d$  to the LES resolved field  $\bar{u}$ :

$$u^< = G_d(\bar{u}), \quad u^> = \bar{u} - u^< = (1 - G_d)(\bar{u}) \quad (38)$$

The four possible combinations are illustrated below taking the Smagorinsky model (26) as an example.

- The Large-Large model, which corresponds to the original model (26) in which both parts are computed using the full resolved field, leading to very poor localness properties in terms of wave number
- The Large-Small model proposed by Hughes, in which the subgrid viscosity is evaluated using the full resolved field, while the velocity gradient tensor is restricted to  $u^>(x, t)$ :

$$\tau = -2(C_S \Delta)^2 |\bar{S}| S^>, \quad S^> \equiv \frac{1}{2} (\nabla u^> + \nabla^t u^>) \quad (39)$$

- The Small-Small model of Hughes, in which both parts are computed using the small resolved scales only

$$\tau = -2(C_S \Delta)^2 |S^>| S^> \quad (40)$$

- The Small-Large model, which is strictly equivalent to the filtered

model concept developed by Ducros on the grounds of the structure function model and further extended by Sagaut et al. [36]:

$$\tau = -2(C_S \Delta)^2 |S^>| \bar{S} \quad (41)$$

The Small-Small and Large-Small models share the property that, if the  $u^>$  and  $u^<$  are orthogonal, the subgrid energy drain will acts on the  $u^>$  component only. In the case of a Fourier spectral implementation, this orthogonality property was shown to yield spurious energy pile-up in the  $u^<$  component due to the fact that non-local energy transfers toward subgrid modes are not taken into account. These two models can also be easily recast as hyperviscosity models assuming the following differential approximation of the test filter  $G_d$  is valid

$$G_d(\bar{u})(x) = \bar{u} - \alpha \Delta^{2p} \nabla^{2p} \bar{u} + o(\Delta^{2p}) \quad (42)$$

where  $\alpha$  and  $p$  are filter-dependent parameters, which leads to

$$u^> \simeq \alpha \Delta^{2p} \nabla^{2p} \bar{u} \quad (43)$$

yielding the following approximations

$$\tau = -2\alpha C_S^2 \Delta^{2(p+1)} |\bar{S}| \nabla^{2p}(\bar{S}) \quad \text{Large-Small model} \quad (44)$$

$$\tau = -2\alpha^2 C_S^2 \Delta^{2(2p+1)} |\nabla^{2p}(\bar{S})| \nabla^{2p}(\bar{S}) \quad \text{Large-Small model} \quad (45)$$

These new formulations make the improved spectral localness properties clearer and show how they are governed by those of the test filter. Generalized versions based on a filtering approach have been proposed by Vreman [47].

#### 2.4.2. Structural subgrid scale models

The structural models aim at predicting the subgrid scales (or the subgrid tensor) directly, rather than recovering their effects on the resolved scales through the use of a forcing term. Obviously, an accurate prediction of the subgrid scales would lead to a satisfactory estimation of the forcing term  $\mathcal{F}_{LES}$ .

While the distinction between the single- and the twice-filtered Navier-Stokes model was not important in the functional modelling case, it is a central feature in the structural model case. Looking at Eq.(11), it is clear that only the  $u'$  field can be reconstructed on the computational grid. As a consequence, one can distinguish between two general classes of structural models:

- (1) *Models and methods for reconstructing  $u'$  only.* This approach was coined as the *soft deconvolution* problem by Adams, and makes it possible to evaluate the term  $F_1$  in Eq.(12). Since interactions with the field  $u''$  are not taken into account, these models must be supplemented by a secondary model of structural type which will account for  $F_2$  and  $F_3$  in Eq.(12), leading to the definition of *mixed models*, also called linear combination models. This combination is also supported by physical arguments developed by Shao et al., who found in a priori tests that terms  $F_0$  and  $F_1$  are rapid terms (i.e. terms which react quickly to changes in the resolved field) which carry most of the information tied to anisotropy of resolved scales, while  $F_2$  and  $F_3$  are slow terms mostly related to an isotropic energy cascade.
- (2) *Models and methods for estimating both  $u'$  and  $u''$ .* An auxiliary computational grid is now introduced to capture  $u''$  or its surrogate. This approach can be referred to as a *full reconstruction approach*.

**Soft deconvolution models** All models belonging to this family rely on a partial inversion of the first filtering step introduced within the twice-filtered Navier-Stokes equations LES model framework. The purpose is to evaluate the field  $u^* \simeq \tilde{u} \equiv \tilde{u} + u'$  using  $\tilde{u}$  as a starting point and then to use it as a predictor of the whole resolvable field  $\tilde{u}$ , yielding the following expression for generalized soft deconvolution models:

$$\tau \approx \widetilde{u^* \otimes u^*} - \tilde{u}^* \otimes \tilde{u}^* \quad (46)$$

Many strategies have been developed, among which:

- (1) The iterative deconvolution, as advocated by Stolz and Adams [40, 41, 42]. Writing  $\tilde{u} = \overline{G} \star \tilde{u}$ , one obtains

$$\tilde{u} = [I - (I - \overline{G})]^{-1} \tilde{u} = \sum_{p=0, +\infty} (I - \overline{G})^p \tilde{u} \quad (47)$$

The approximate solution  $u^*$  is obtained using a truncated expansion

$$u^* = \sum_{p=0, N} (I - \overline{G})^p \tilde{u} \quad (48)$$

with  $N \leq 5$  in practice. The lowest-order expansion ( $N = 0$ ) corresponds to the model proposed by Bardina referred to as the scale-similarity model :

$$u^* = \tilde{u} \longrightarrow F_1 = \overline{\tilde{u} \otimes \tilde{u}} - \overline{\tilde{u}} \otimes \overline{\tilde{u}} \quad (49)$$

- (2) The Taylor series expansion approach, which relies on a differential approximation of the convolution filter.

Recalling that (in 1D)

$$\overline{u} = \int \overline{G}(x - y) u(y) dy \quad (50)$$

and introducing the Taylor series expansion of  $u(y)$

$$u(y) = u(x) + \sum_{k=1, +\infty} \frac{(y - x)^k}{k!} \frac{d^k}{dx^k} u(x) \quad (51)$$

one obtains

$$\overline{u}(x) = \left( I + \sum_{k=1, +\infty} \frac{(-1)^k}{k!} M_k \frac{d^k}{dx^k} \right) u(x) \quad (52)$$

where  $M_k$  is the  $k$ th moment of the filter kernel  $\overline{G}$ :

$$M_k = \int z^k \overline{G}(z) dz$$

For Gaussian and top hat filters, which are symmetric, non-vanishing moments are such that  $M_k = O(\Delta^k)$ . The deconvolution can therefore be written as

$$u(x) = \left( I + \sum_{k=1, +\infty} \frac{(-1)^k}{k!} M_k \frac{d^k}{dx^k} \right)^{-1} \overline{u} \quad (53)$$

The approximate inverse  $u^*$  is obtained using a truncated Taylor series expansion:

$$u^*(x) = \left( I + \sum_{k=1, N} \frac{(-1)^k}{k!} M_k \frac{d^k}{d^k} \right)^{-1} \tilde{u} \quad (54)$$

The computation of the inverse differential operator can be achieved in different ways. A first solution is to discretize it and to inverse it numerically. A second (and much more common) solution is to develop it using another truncated Taylor series expansion :  $(1 + \epsilon)^{-1} = 1 - \epsilon + \epsilon^2 \dots$ . Restricting this development to second-order terms (i.e. up to  $O(\Delta^2)$  terms), one recovers the following well-known model (referred to as Clark model, gradient model or tensor diffusivity model):

$$F_{1ij} = \frac{1}{12} \Delta^2 \frac{\partial \tilde{u}_i}{\partial x_k} \frac{\partial \tilde{u}_j}{\partial x_k} \quad (55)$$

This model can also be derived performing a Taylor series expansion of the subgrid stresses. A finite-difference equivalent model referred to as the velocity increment model was proposed by Brun and Friedrich.

All soft-deconvolution models are under-dissipative in the sense that they do not prevent energy pile-up in the resolved scales. This is consistent with the fact that they do not account for interaction with "true" subgrid scales represented by  $u''$  field. In the case of the tensor diffusivity model, this lack of dissipation is associated to anti-diffusive properties along proper axes of  $\tilde{S}$  associated to negative eigenvalues.

**Full reconstruction of subgrid scales** These models require the definition of an auxiliary fine grid with characteristic mesh size  $h' < h$  on which the field  $u''$  will be reconstructed. They can be recast within the general framework of multilevel techniques. The original LES grid with mesh size  $h$  is then referred to as the coarse grid (or coarse resolution level). This new resolution level is represented using another filtering step within the filtered Navier-Stokes equations framework. The common structure of all these methods is the following

- (1) Extend the coarse grid solution  $\tilde{u}$  on the fine grid. This is achieved using an interpolation step, which can be supplemented by a deconvolution step to recover  $\tilde{u}$ .

- (2) Reconstruct the subgrid scale field  $u''$  on the fine grid, and add it to  $\bar{u}$  to get  $u$
- (3) Compute the non-linear term  $F(u, u)$  on the fine grid
- (4) Restrict it at the coarse resolution level to obtain  $\widetilde{F(u, u)}$ . This step can be implemented as a projection or a combination of a filtering step and a projection step.

The gain in terms of computational time with respect to a usual LES computation performed on the fine grid is achieved using at least one among the two techniques listed below (see [35, 6] for details):

- Use a cheap method (i.e. cheaper than solving the Navier-Stokes equations) to evaluate  $u''$  on the fine grid. This can be done using many methods, e.g. : (i) fractal interpolation of the resolved field (ii) kinematic extrapolation based on an estimate of the production term.
- Define a cycling strategy between the two resolution levels, i.e. freeze the  $u''$  on the fine grid for some time. This time can be prescribed using phenomenological arguments or can be computed using a priori error estimates. Further cost reduction can be achieved using a set of embedded resolution level (Terracol et al. [43, 44] used up to 3 resolution levels in the case of a compressible plane channel flow).

### 3. Rewriting LES as a Multiscale/Multilevel problem

The scale separation concept has been extensively introduced and discussed in the previous section. It is now proposed to extend this concept to the case which consists to introduce several (not only one) filtering (or representation) levels of the solution. As it will be further detailed, the concept of decomposition of the flow variables between resolved and unresolved parts will not be limited to a a scale separation between large and small scales. Indeed, the more general context of multilevel/multiresolution methods will also be investigated.

#### 3.1. A $N$ -level multiscale turbulent field decomposition

As a first step, the particular case of a multiscale decomposition of the flow variables has to be described. Similarly to what is done in classical Large-Eddy Simulation, different filtering levels of the flow variables are introduced through the use of some filtering operators denoted by  $G_n$ ,  $1 < n < N$ , acting as a low-pass frequency filters on the solution, and

associated to their respective cutoff lengthscale  $\Delta^{(n)}$ .

The application of the filtering operator  $G_n$  on the variable  $u$  is then formally defined by a convolution product<sup>d</sup>:

$$(G_n \star u)(x, t) = \int_{\Omega} G_n(\Delta^{(n)}, x - \xi) u(\xi, t) d\xi \quad (56)$$

In the following, it will be assumed that the hierarchy of *primary* filters  $G_n$  is chosen such that growing values of the parameter  $n$  correspond to coarser and coarser representations of the flow variables. This is equivalent to say that the respective cutoff lengthscales  $\Delta^{(n)}$  of the filters  $G_n$  are increasing with  $n$ , *i.e.*  $\Delta^{(n+1)} > \Delta^{(n)}$ . For the particular case  $n = 0$ , it will be imposed that  $G_0 = Id$ .

Another filtering operator  $\mathcal{G}_m^n$  has then to be introduced, which results from the successive application of the primary filters  $G_m$  to  $G_n$ :

$$\mathcal{G}_m^n(\cdot) = G_n \star G_{n-1} \star \dots \star G_{m+1} \star G_m \star (\cdot) \quad (57)$$

This definition yields to a hierarchy of filtering operators  $\{\mathcal{G}_1^n\}_{n=1, N}$ , which will be used to perform the scale separation at each level  $n$ . In the following, these filtering operators  $\mathcal{G}_1^n$  will be referred to as *hierarchical* or *combined* filters, and generally differ<sup>e</sup> from the *primary* filters  $G_n$ . The filtered (resolved) variable at each level  $n$  is then defined as:

$$\begin{aligned} \bar{u}^{(n)} &= \mathcal{G}_1^n(u) \\ &= \mathcal{G}_0^n(u) \\ &= G_n \star G_{n-1} \star \dots \star G_1 \star u \end{aligned} \quad (58)$$

The cutoff lengthscale<sup>f</sup> of the filter  $\mathcal{G}_1^n$  will denoted by  $\bar{\Delta}^{(n)}$ . The filtered variable  $\bar{u}^{(n)}$  then formally corresponds to a representation of the wavenumbers  $k < k_n$ , with  $k_n = \pi/\bar{\Delta}^{(n)}$  the cutoff wavenumber associated to the filter  $\mathcal{G}_1^n$ . In a similar way,  $\bar{u}^{(n)}$  corresponds to a representation of turbulent scales larger than  $\bar{\Delta}^{(n)}$ .

<sup>d</sup>As it is usually the case in Large-Eddy Simulation, the cutoff length  $\Delta^{(n)}$  is assumed to be constant in both space and time, to simplify the following developments. Similarly, no explicit dependency of the filter kernel  $G_n$  with time will be considered.

<sup>e</sup>The identity  $\mathcal{G}_1^n = G_n$  is however verified for the ideal case of a sharp separation between large and small scales at each level  $n$ , when the primary filters are all some sharp cutoff filters.

<sup>f</sup>It is to be noted here that the cutoff lengthscale of the combined filter  $\mathcal{G}_1^n$  generally differs from the one of the primary filter  $G_n$ , *i.e.*  $\bar{\Delta}^{(n)} \neq \Delta^{(n)}$ . The equality is however verified when Reynolds filtering operators are considered as primary filters

It is now convenient to introduce the quantity  $\delta u^{(l)}$ ,  $1 < l < N - 1$ , which is associated to the wavenumbers  $k_{l+1} < k < k_l$ . This quantity will be referred to as the *detail* between the two successive levels  $l$  and  $l + 1$ , and represents the complement (*frequency complement*) of information between these two representation levels. It is evaluated as:

$$\begin{aligned}\delta u^{(l)} &= \bar{u}^{(l)} - \bar{u}^{(l+1)} \\ &= (Id - G_{l+1}) \star \bar{u}^{(l)} \\ &= (\mathcal{G}_1^l - \mathcal{G}_1^{l+1}) u\end{aligned}\tag{59}$$

In the particular context of Large-Eddy Simulation, the following decomposition of the variable  $u$  is considered:

$$u = \bar{u}^{(1)} + u'\tag{60}$$

where  $u' = \delta u^{(0)}$ .

In this case, the simulation is restricted to the description of the filtered field  $\bar{u}^{(1)}$ , while the effects of the unresolved subgrid scales carried by  $u'$  is accounted for thanks to the use of a subgrid model. From the definition of the details, the resolved field at the finest level  $\bar{u}^{(1)}$  can be expressed as a function (denoted by  $\mathcal{M}_{\mathcal{L}}$ ) of the resolved field at a given level  $n > 1$ :

$$\begin{aligned}\bar{u}^{(1)} &= \mathcal{M}_{\mathcal{L}}(\bar{u}^{(n)}, \delta u^{(n-1)}, \dots, \delta u^{(1)}) \\ &= \bar{u}^{(n)} + \sum_{l=1}^{n-1} \delta u^{(l)}\end{aligned}\tag{61}$$

This relation shows that the filtered variable at the finest resolution level can thus be reconstructed thanks to its multilevel (multiscale) decomposition by summation of all its components at coarser filtering levels.

Such a multilevel decomposition is illustrated in the spectral space on figure 1, in the simple case in which the primary filters  $G_n$  are sharp cut-off filters with respective cut-off wavenumbers  $k_n$ .

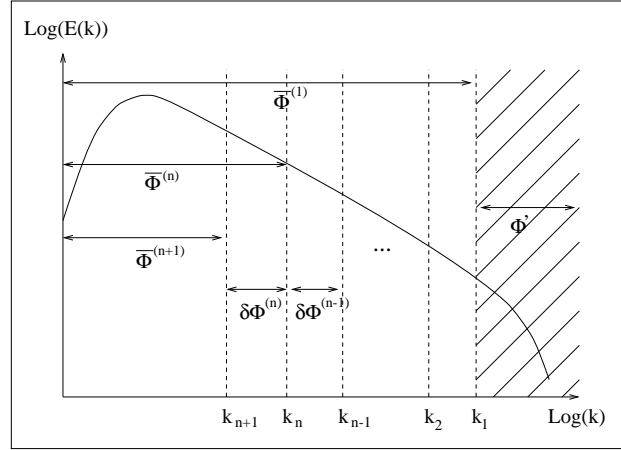


Fig. 1. Multilevel decomposition of the turbulent field (sharp cut-off filters).

Obviously, the simulation tends to a direct simulation when  $\Delta^{(1)} \rightarrow 0$ , *i.e.*  $\bar{u}^{(1)} \rightarrow u$ . As it will be detailed in the following, the main idea of the multilevel will be - without increasing the cost of the simulation - to consider some sufficiently small values of  $\Delta^{(1)}$  to use a simple subgrid closure to represent the effect of the scales associated to  $u'$ , and minimize the errors due to this parametrization.

### 3.2. Corresponding Navier-Stokes-based governing equations

The multilevel decomposition can be formally applied to any set of variables and equations. We will however restrict ourselves to the framework of turbulence simulation, and thus consider the Navier-Stokes equations. For a sake of simplicity in the developments, the incompressible framework will be considered here. The extension to the compressible case is similar to the one performed in classical Large-Eddy Simulation.

The filtered equations at any filtering level  $n$  are obtained by applying the filtering operator  $\mathcal{G}_1^n$  to the Navier-Stokes equations written for a Newtonian incompressible fluid. Under the assumption (discussed in section 2) of commutation between the filtering operator and the time and spatial

derivatives, the following set of filtered equations is obtained:

$$\begin{aligned} \nabla \cdot \bar{u}^{(n)} &= 0 \\ \frac{\partial}{\partial t} \bar{u}^{(n)} + \nabla \cdot \left( \bar{u}^{(n)} \otimes \bar{u}^{(n)} \right) &= -\nabla \bar{p}^{(n)} + \nu \nabla^2 \bar{u}^{(n)} - \nabla \cdot \tau^{(n)} \end{aligned} \quad (62)$$

In this expression,  $\tau^{(n)}$  is the subgrid stress-tensor of the level  $n$ , arising from the non-linearity of the Navier-Stokes equations, defined as:

$$\tau^{(n)} = \overline{u \otimes u}^{(n)} - \bar{u}^{(n)} \otimes \bar{u}^{(n)} \quad (63)$$

As it is the case in classical Large-Eddy Simulation, this term cannot be directly computed at the filtering level  $n$ , since the unfiltered velocity field  $u$  appears in its expression. A specific closure is thus needed for this term to close the system of equations (62). The next section of this chapter will be devoted to some existing possible parametrizations for this term.

It is to be noted that an evolution equation can also be obtained for the details between two consecutive levels  $n$  and  $n + 1$ . Indeed, by simply subtracting the filtered Navier-Stokes equations at the coarser level  $n + 1$  from equations (62), and since  $\bar{u}^{(n)} = \bar{u}^{(n+1)} + \delta u^{(n)}$  and  $\bar{p}^{(n)} = \bar{p}^{(n+1)} + \delta p^{(n)}$ , the following system is derived for the details  $\delta u^{(n)}$  and  $\delta p^{(n)}$ :

$$\begin{aligned} \nabla \cdot (\delta u^{(n)}) &= 0 \\ \frac{\partial}{\partial t} \delta u^{(n)} + \nabla \cdot (\delta u^{(n)} \otimes \delta u^{(n)} + \delta u^{(n)} \otimes \bar{u}^{(n+1)} + \bar{u}^{(n+1)} \otimes \delta u^{(n)}) & \\ &= -\nabla \delta p^{(n)} + \nu \nabla^2 \delta u^{(n)} - \nabla \cdot (\tau^{(n)} - \tau^{(n+1)}) \end{aligned} \quad (64)$$

This system will be the main basis of the NLDE (Non-Linear Disturbance Equations) approach [25], which allows to get a reconstruction of the turbulent fluctuations around a given mean flow.

### 3.3. The closure problem

As it has been shown in the previous section, the application of the hierarchical filter  $\mathcal{G}_1^n$  on the Navier-Stokes equations leads to some extra terms in the filtered equations which are not directly computable at this level. As in the classical Large-Eddy Simulation terminology, these terms will be referred to as the *subgrid* terms from level  $n$ . At each filtering level, a mathematical closure has thus to be considered for the subgrid stress-tensor  $\tau^{(n)}$ . Several solutions exist to perform such a closure. This section deals with a brief survey of existing parametrizations for the subgrid-stress tensor  $\tau^{(n)}$ . First, the simplest case which uses a classical subgrid model at each level  $n$  of filtering of the solution will be presented. It is equivalent to account for

the subgrid scales (corresponding to the wavenumbers  $k > k_n$ ) in a statistical way. This point is illustrated in Figure 2.

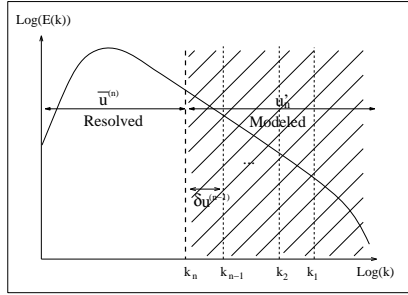


Fig. 2. "Standard" parametrization of the subgrid scales (sharp cut-off filter).

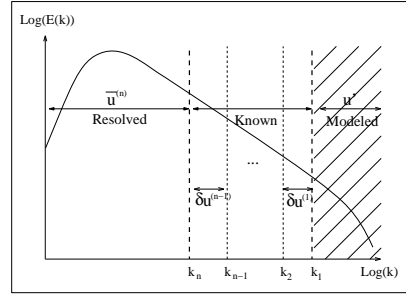


Fig. 3. Multilevel parametrization of the subgrid scales (sharp cut-off filter).

However, for  $n > 1$ , a part of the subgrid information related to the level  $n$  is known, since it is explicitly resolved at the finer filtering levels  $l \in [1, n - 1]$ . Indeed, this information is contained in the details of the finer levels, and it thus appears possible to directly use it in the computation of the subgrid terms at level  $n$ . This point is illustrated in Figure 3, and is the basic idea for the development of several specific multilevel closures, which will be described in this section. It is to be noted that these specific closures rely on an extension of the Germano's identity to the case of a  $n$ -scale decomposition.

### 3.3.1. Use of a "classical" subgrid model

This kind of parametrization remains the most simple to implement. Here, a classical subgrid model (see section 2 for a survey) is retained at each filtering level  $n$ . The subgrid stresses at each level are then expressed as a function of the resolved variables at this level:

$$\tau^{(n)} \simeq \mathcal{M}_{sgs} \left( \overline{\Delta}^{(n)}, \overline{u}^{(n)} \right) \quad (65)$$

where  $\mathcal{M}_{sgs}$  stands for one of the subgrid models presented in section 2. While this kind of parametrization for the subgrid terms remains obviously the simplest one to implement, it relies on the fact that all the scales which are not resolved at the level  $n$  are represented through the use of a statistical model. It is then obvious to think that such a model has a decreasing accuracy when  $n$  (equivalently  $\overline{\Delta}^{(n)}$ ) increases, *i.e.* when the quantity of

subgrid information to account for increases. Indeed, for too large values of  $n$ , the assumptions considered in the development of the subgrid models<sup>§</sup> may be dramatically violated, leading to a high level of error in the model. For this reason, some appropriate multilevel models have been developed by several authors. One of the common basis of these models is the generalization of Germano's identity to the multilevel framework, which is detailed in the next section.

### 3.3.2. Multilevel generalization of the Germano's identity

From the expression of the subgrid stress-tensor at the filtering level  $n$ , we can write:

$$G_{n+1} \star \tau^{(n)} = \overline{u \otimes u}^{(n+1)} - G_{n+1} \star (\overline{u}^{(n)} \otimes \overline{u}^{(n)}) \quad (66)$$

We then obtain the following relation:

$$\tau^{(n+1)} - G_{n+1} \star \tau^{(n)} = \mathcal{L}^{(n)} \quad (67)$$

where the tensor  $\mathcal{L}^{(n)}$  can be directly computed from the resolved field at the two successive levels  $n$  and  $n + 1$ :

$$\mathcal{L}^{(n)} = G_{n+1} \star (\overline{u}^{(n)} \otimes \overline{u}^{(n)}) - \overline{u}^{(n+1)} \otimes \overline{u}^{(n+1)} \quad (68)$$

Relation (67) is a multilevel formulation of the well-known Germano's identity [16]. Indeed, with  $n = 1$ , and with the notations  $\overline{\phi} = \overline{\phi}^{(1)}$  and  $\widetilde{\phi} = G_2 \star \phi$ , we get the classical expression of this identity, similar to (34):

$$\mathcal{L} = T - \widetilde{\tau} \quad (69)$$

where we recall that:

$$\tau = \overline{u \otimes u} - \overline{u} \otimes \overline{u} \quad (70)$$

$$T = \widetilde{\overline{u \otimes u}} - \widetilde{\overline{u}} \otimes \widetilde{\overline{u}} \quad (71)$$

$$\mathcal{L} = \widetilde{\overline{u \otimes u}} - \widetilde{\overline{u}} \otimes \widetilde{\overline{u}} \quad (72)$$

By recurrence, we also get from (67) the following expression for the subgrid-stress tensor from a level  $n > 1$ :

$$\tau^{(n)} = \mathcal{G}_2^n \left( \tau^{(1)} \right) + \sum_{m=1}^{n-1} \mathcal{G}_{m+2}^n \left( \mathcal{L}^{(m)} \right) \quad (73)$$

<sup>§</sup>Generally isotropy and homogeneity of the unresolved scales

where we impose that  $\mathcal{G}_m^l = Id$  for  $m > l$ .

It thus appears from this relation that the subgrid terms from a given level  $n$  can be directly computed if the subgrid term from the finest filtering level  $\tau^{(1)}$  is known. The consequence is that the only resulting errors in the parametrization of  $\tau^{(n)}$  are relative to those done when modelling  $\tau^{(1)}$ . In the following, relation (73) will be referred to as the *generalized Germano's identity*, which is one of the major relation between the subgrid terms at different filtering levels.

### 3.3.3. Specific multilevel closures

In this section, two specific closures, well suited to the multilevel framework, will be described. The basic common idea of these closures is, at a level  $n > 1$ , to use the information resolved on finer levels from a deterministic way rather than modelling it from a statistical way as it would be the case with one of the standard LES parametrization.

- A first closure can be derived directly from the generalized Germano's identity. The subgrid terms at any level  $n > 1$  are thus expressed by using directly the relation (73) and by considering a "usual" closure for the subgrid terms from the finest representation level<sup>h</sup> ( $n = 1$ ). The expression of the subgrid-stress tensor at any level  $n > 1$  then reads:

$$\begin{aligned} \tau^{(n)} &\simeq \mathcal{G}_2^n \left( \mathcal{M}_{sgs} \left( \overline{\Delta}^{(1)}, \overline{u}^{(1)} \right) \right) \\ &+ \sum_{m=1}^{n-1} \mathcal{G}_{m+2}^n \left( G_{m+1} \star \left( \overline{u}^{(m)} \otimes \overline{u}^{(m)} \right) - \overline{u}^{(m+1)} \otimes \overline{u}^{(m+1)} \right) \end{aligned} \quad (74)$$

Here, it should be noticed that no particular *a priori* assumption is made about the form or intrinsic nature of the subgrid terms (particularly, the backscatter phenomenon is not prohibited), except for the term  $\tau^{(1)}$ .

Several implementations of this closure can be found in the literature, leading to some different classes of methods. These various methods differ by the way to perform practically the multiscale decomposition, the number of levels which are considered, and some additive hypothesis/simplifications of the expression (74). Section 3.4 presents how the main multilevel methods are derived in practice.

<sup>h</sup>This closure should then be of a reliable accuracy since the flow should satisfy the usual LES assumptions at this resolution level

- The second possible closure relies on an extension of the dynamic mixed closure of Zang *et al.* [49] to the case of a  $N$ -level scale decomposition. This model, proposed by Terracol *et al.* [43], relies on a specific form of the scale-similarity term at a given level  $n > 1$ , which includes a contribution relative to the information resolved at the finer levels. While all the original developments were carried out in the compressible case, only the incompressible one will be detailed here to be consistent with the previous developments.

First of all, the following decomposition of the velocity field is introduced:

$$u = \bar{u}^{(n)} + \sum_{l=1}^{n-1} \delta u^{(l)} + u' \quad (75)$$

where  $u' = \delta u^{(0)}$ . This decomposition is then introduced directly in the expression of the subgrid term  $\tau^{(n)}$  from level  $n$ , leading to the following decomposition, similar to the Germano's consistent decomposition:

$$\tau^{(n)} = L^{(n)} + C^{(n)} + R^{(n)} \quad (76)$$

where the three terms  $L^{(n)}$ ,  $C^{(n)}$ , and  $R^{(n)}$  read:

$$L^{(n)} = \mathcal{G}_1^n \left( \left( \bar{u}^{(n)} + \sum_{l=1}^{n-1} \delta u^{(l)} \right) \otimes \left( \bar{u}^{(n)} + \sum_{l=1}^{n-1} \delta u^{(l)} \right) \right) \quad (77)$$

$$- \mathcal{G}_1^n \left( \bar{u}^{(n)} + \sum_{l=1}^{n-1} \delta u^{(l)} \right) \otimes \mathcal{G}_1^n \left( \bar{u}^{(n)} + \sum_{l=1}^{n-1} \delta u^{(l)} \right)$$

$$C^{(n)} = \mathcal{G}_1^n \left( \left( \bar{u}^{(n)} + \sum_{l=1}^{n-1} \delta u^{(l)} \right) \otimes u' \right) \quad (78)$$

$$- \mathcal{G}_1^n \left( \bar{u}^{(n)} + \sum_{l=1}^{n-1} \delta u^{(l)} \right) \otimes \mathcal{G}_1^n (u')$$

$$+ \mathcal{G}_1^n \left( u' \otimes \left( \bar{u}^{(n)} + \sum_{l=1}^{n-1} \delta u^{(l)} \right) \right)$$

$$- \mathcal{G}_1^n (u') \otimes \mathcal{G}_1^n \left( \bar{u}^{(n)} + \sum_{l=1}^{n-1} \delta u^{(l)} \right)$$

$$R^{(n)} = \mathcal{G}_1^n (u' \otimes u') - \mathcal{G}_1^n (u') \otimes \mathcal{G}_1^n (u') \quad (79)$$

These three terms refer respectively to the resolved, cross, and Reynolds stress tensors of the subgrid-stress tensor:

- $L^{(n)}$  is the resolvable part of  $\tau^{(n)}$ , and appears as an extension of Bardina’s scale similarity model to the multilevel case. It represents the large scales interactions, and in addition the interactions between large scales and the small scales resolved on the finer levels, and interactions between these ”resolved subgrid scales” themselves. This part of the subgrid stress-tensor contains all the deterministic information that can be directly computed.
- $C^{(n)}$  is the cross-term tensor, which represents interactions between the large scales and the unresolved subgrid scales, and between resolved and unresolved subgrid scales.
- $R^{(n)}$  is the classical Reynolds stress-tensor, which represents the interactions between the unresolved subgrid scales.

Since  $L^{(n)}$  can be directly computed from the resolved field, it is proposed to perform a direct computation of this term, while modelling only the two other terms  $C^{(n)}$  and  $R^{(n)}$  from a statistical way. Such a parametrization of these two terms can be achieved thanks to a classical Smagorinsky model with an appropriate value of the Smagorinsky coefficient, obtained by mean of the dynamic procedure.

Similarly to what was proposed by Zang *et al.* [49], the subgrid stress tensor at two consecutive filtering levels  $n$  and  $n + 1$  are expressed as:

$$\tau^{(n)} = L^{(n)} - 2C_d^{(n)} \left( \Delta^{(n)} \right)^2 \left| \overline{S}^{(n)} \right| \overline{S}^{(n)} \quad (80)$$

$$\tau^{(n+1)} = L^{T(n)} - 2C_d^{(n)} \left( \Delta^{(n+1)} \right)^2 \left| \overline{S}^{(n+1)} \right| \overline{S}^{(n+1)} \quad (81)$$

where  $\left| \overline{S}^{(n)} \right| = \sqrt{2 \overline{S}^{(n)} : \overline{S}^{(n)}}$ .

As in the usual dynamic approach, it is assumed<sup>i</sup> that  $C_d^{(n)}$  is the same for all the wavenumbers between  $k_{n+1}$  and  $k_n$ .

The term  $L^{T(n)}$  is obtained<sup>j</sup> similarly to  $L^{(n)}$  by introducing the velocity

<sup>i</sup>This assumption is however only needed at the finest level  $n = 1$ . Indeed, for  $n > 1$ , another procedure can be applied, in which two different coefficients  $C_d^{(n)}$  and  $C_d^{(n+1)}$  are considered, and are computed recursively from the finest to the coarsest resolution level.

<sup>j</sup>It should be noted that  $L^{T(n)} \neq L^{(n+1)}$ . Indeed this last term is obtained from the the velocity field decomposition at level  $n + 1$  (not  $n$ ).

field decomposition (75) at level  $n$  into the expression of  $\tau^{(n+1)}$ :

$$\begin{aligned} L^{T(n)} &= \mathcal{G}_1^{n+1} \left( \left( \bar{u}^{(n)} + \sum_{l=1}^{n-1} \delta u^{(n)} \right) \otimes \left( \bar{u}^{(n)} + \sum_{l=1}^{n-1} \delta u^{(n)} \right) \right) \\ &\quad - \mathcal{G}_1^{n+1} \left( \bar{u}^{(n)} + \sum_{l=1}^{n-1} \delta u^{(n)} \right) \otimes \mathcal{G}_1^{n+1} \left( \bar{u}^{(n)} + \sum_{l=1}^{n-1} \delta u^{(n)} \right) \end{aligned} \quad (82)$$

By applying the Germano's identity (67) to the two expressions (80) and (81), the following relation is derived:

$$\mathcal{L}^{(n)} = \left( L^{T(n)} - G_{n+1} \star L^{(n)} \right) - 2C_d^{(n)} M^{(n)} \quad (83)$$

where:

$$M^{(n)} = \left( \Delta^{(n+1)} \right)^2 \left| \bar{S}^{(n+1)} \right| \bar{S}^{(n+1)} - \left( \Delta^{(n)} \right)^2 G_{n+1} \star \left( \left| \bar{S}^{(n)} \right| \bar{S}^{(n)} \right) \quad (84)$$

An optimized value of the coefficient  $C_d^{(n)}$  is then obtained by a least-square minimization of the residual of relation (83):

$$C_d^{(n)} = - \frac{\mathcal{L}^{(n)} - \left( L^{T(n)} - G_{n+1} \star L^{(n)} \right)}{2M^{(n)} : M^{(n)}} \quad (85)$$

It is to be noted that, as it is the case for the classical dynamic model, the values obtained for this coefficient at each level are much lower (roughly one order of magnitude) than the values commonly retained for the Smagorinsky constant. This is due to the presence of the scale-similarity term  $L^{(n)}$  which exhibits a high degree of correlation with the real subgrid term  $\tau^{(n)}$ .

A second remark is that this model, exactly as the classical dynamic model, is subject to some numerical instabilities that can arise when too important variations or intense negative values of the parameter  $C_d^{(n)}$  are obtained. For this reason, some stabilization techniques such as volume/plane averaging or clipping of the coefficient itself or of its numerator and denominator parts have to be carried out.

### 3.4. Typology of existing methods

Several multilevel methods can be found in literature, which can be classified in different subclasses, depending on the nature of the primary "filtering" operators  $G_n$ . This section is a proposal of a possible classification of some existing multilevel methods, together with their brief description.

First of all, the choice of the primary operators  $G_n$  has to be discussed. Depending on this choice, two main classes of multiscale decomposition arise:

- (1) To consider that the filtering operation is carried out by applying low-pass filters (in wavenumber) on the flow variables at each level  $n$ , as the ones commonly used in Large-Eddy Simulation. This leads to the multiscale representation of the aerodynamic variables described in the previous sections.

Three general types of method, belonging to this first class of multiscale decomposition can be cited:

- The deconvolution-like methods [40, ?, ?, ?, ?, ?, ?], which propose to perform an approximate reconstruction of some scales smaller than the resolved scales in order to compute explicitly the subgrid terms. This is achieved by introducing two filtering levels. With the former notations, the "resolved" field will be  $\bar{u}^{(2)}$ , while the field at the finest resolution level  $\bar{u}^{(1)}$  is only used (and approximated) to build the subgrid terms.
- The "improved" functional models based on an additional separation between large and small resolved scales, such as the ones based on the removal of the mean flow, the Variational Multiscale Model [18, 19, 20], and filtered models. In all these approaches, a classical functional model such as the Smagorinsky model is modified such that different combinations of resolved scales are used to compute the shear-stress tensor and the subgrid viscosity.
- The multilevel methods based on the use of a hierarchical representation of the solution, and obtained in practice thanks to the use of a hierarchy of computational grids with different resolutions, for instance by using a *multigrid*<sup>k</sup> algorithm or the Adaptive Mesh Refinement (AMR) technique.

In this case - as it will be detailed in the next sections - the scale decomposition is obtained implicitly by the use of several grid levels, with different grid resolutions. Each grid level then naturally introduces its own cutoff lengthscale (the grid Nyquist cutoff), and the effective "filtering" at each level results from a combination of this natural cutoff, the numerical scheme, and a possible additional explicit filtering, as it was specified in the first part of this chapter.

---

<sup>k</sup>The multigrid terminology is used here referring to its primary definition "use of different computational grids", and should not be compared to the multigrid methods developed for convergence acceleration in steady CFD algorithms, and which make use of specific numerical treatments.

- (2) To consider the particular case of a two-level decomposition of the flow variables between a filtered (LES) part, and an averaged (RANS) part. This yields to the framework of the so-called RANS/LES hybrid approaches, which are of growing interest for practical applications of the LES technique. In this case, a classical low-pass filter is considered at the finest resolution level ( $n = 1$ ), while the "coarse" resolution level ( $n = 2$ ) is defined through the use of a Reynolds averaging operator. It should be noticed that in this case, the multilevel method is then extended to the *multiresolution* framework since the different resolution levels are obtained thanks to different kind of representations/resolutions of the flow.

It thus appear that the multilevel methods in Large-Eddy Simulation can be divided into four subclasses. However, one common point of all these methods is that they all aim at increasing (locally or globally) the accuracy of the simulation, while keeping affordable computational costs. Two main applications then arise: i) increase accuracy at a constant computational cost; ii) decrease the computational cost at a constant accuracy.

The case of the RANS/LES hybrid methods is a major (and rich) topic which will not be detailed in this chapter, limited to multilevel LES. For a description of hybrid RANS/LES strategies, the reader is referred to [35].

The deconvolution-like methods belong to the structural subgrid scale closures, and have thus been extensively described in section 2.4. In that case, because only two filtering levels were defined, some more simple notations were retained: the resolved field (at level number 2) is denoted by  $\tilde{u}$ . The approximate inverse (at level number 1) is denoted by  $u^*$ .

Similarly, the improvements of functional models based on an additional scale separation have been detailed in section 2.4, where the resolved field  $\bar{u}$  is  $\bar{u}^{(1)}$ , the large resolved scales  $u^<$  are equivalent to  $\bar{u}^{(2)}$ , and finally the small resolved scales  $u^>$  are the details between these two filtering levels  $\delta u^{(1)}$ .

The next section will now be devoted to the description of the remaining subclass emerging from the former classification. The case of a multigrid decomposition will thus be considered. The specific problems and possible treatment arising in this case will be analyzed, for both the case of embedded and zonal multigrid strategies.

#### 4. Multilevel LES by use of several grid levels

The concept of multiscale separation has been extensively introduced and discussed in the previous sections, from the continuous point of view. However, for practical applications, an equivalent discrete formalism has to be introduced.

From the discrete point of view, the way to perform the multiscale separation and to define the different filtering levels in practice is highly dependent of the numerical method that is used. Indeed, the decomposition is straightforward when spectral solvers are used. In that case, a simple truncation of the Fourier representation of the flow variables allows to perform the scale separation (when sharp cutoff filters are used), as it was done by several authors (see the Dynamic MultiLevel (DML) approach of Dubois *et al.* [13, 14, 12, 11, 10]).

However, when the computation is performed in physical space, the filtering step is generally more difficult to perform. Some discrete equivalents to the continuous filters have to be developed. Moreover, when using such approximations of the filters, an important feature of the filters is that it has to reduce the complexity of the problem, or equivalently the number of degrees of freedom. This is generally not the case with classical finite-difference approximations relying on Taylor series expansions.

Spectral approaches have a limited field of applications. For that reason, practical computations are often performed in physical space, meaning by the introduction of a discretization grid. As it has been mentioned previously, any grid, with a grid cell size of  $\Delta$  introduces naturally a cutoff lengthscale (referred to as the Nyquist cutoff) equal to  $2\Delta$ , and which represents formally the smallest flow structure that can be resolved on the mesh. Additionally, the numerical scheme also introduces its own cutoff, so that it is thus very hard to define properly what are the effective cutoff lengthscale and filtering operator of the simulation.

Following these observations, the simplest possible way to perform the scale separation in the physical space, while reducing simultaneously the complexity of the solution, relies on the use of different grids with varying characteristic cell sizes between them. With such a strategy, each grid level thus introduces its own filtering of the solution, and the difficult point is then to perform a coupling between the different grids. In practice, such a coupling appears necessary in two main configurations:

- When the different grid levels are embedded, and define a hierarchy of nested grids, an adapted coupling process between the different

grid levels has to be introduced. If the grids are only partially nested (in a sense that will be defined in section 4.1.2), and define a zonal multigrid hierarchy, some coupling interfaces between the different resolution levels are present and require a proper treatment. This remark also stands for the Adaptive Mesh Refinement methods, in which such a zonal multigrid hierarchy is generated dynamically during the computation. The general case of embedded grids is detailed in section 4.1.

- When the different grid levels do not overlap each others, the coupling between them occurs only at an interface. We then have to deal with a multidomain/multilevel approach. This case, and the underlying difficulties, is fully described in section 4.2. More particularly, emphasis will be made to the particular treatment required at the coupling interface between two domains with different grid resolutions.

#### 4.1. Embedded multilevel LES

##### 4.1.1. Fully embedded strategies

The  $N$  different filtering levels considered here correspond to different discretization grids of a (continuous) domain  $\Omega$ . Each grid level will be denoted by  $\Omega_n$ ,  $n = 1..N$ , where  $\Omega_1$  refers to the finest grid, and  $\Omega_N$  to the coarsest one, respectively. Each grid level then defines implicitly a filtering level of the solution, since it can only account for a limited range of scales. The range of grid-resolved scales thus decreases as  $n$  grows, as in the continuous formalism presented in section 3.1. The finest grid  $\Omega_1$  is thus associated to the finest filtering level, and performs implicitly the primary filtering operation  $G_1 \star$ . That is equivalent to say that the continuous filter kernel  $G_1$  is in practice assimilated to the discretization operator on grid  $\Omega_1$ , denoted by  $\mathcal{D}_1$ . For the continuous variable  $u$ , the filtered variable at the finest resolution level is thus defined as:

$$\bar{u}^{(1)} = \mathcal{D}_1(u) \quad (86)$$

In a similar way, each level of the embedded grid hierarchy defines its own filtering level of the solution, as it is illustrated by figure 4.1 in the restricted case of three filtering/grid levels.

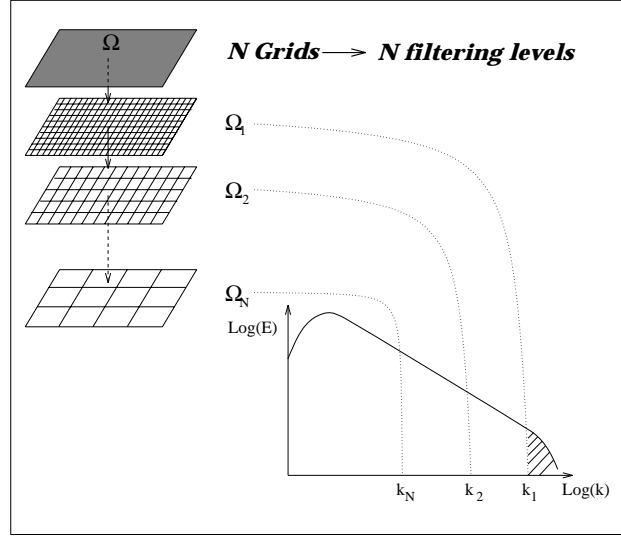


Fig. 4. Practical definition of the filtering levels ( $N = 3$ ).

The definition of the filtered variables at each grid level then require the introduction of *Restriction* operators<sup>1</sup> denoted  $R_n^{n+1}$  and which allow to perform an interpolation of the flow variables resolved at a given level  $\Omega_n$  to the next (coarser) level  $\Omega_{n+1}$ . The filtered variables on the "coarse" ( $n > 1$ ) levels are thus defined recursively from the resolved variables at the finest resolution level, by successive applications of the restriction operators. The filtered variable at level  $n$  is then defined as:

$$\begin{aligned} \bar{u}^{(n)} &= R_{n-1}^n \bar{u}^{(n-1)} \\ &= \underbrace{(R_{n-1}^n \circ R_{n-2}^{n-1} \circ \dots \circ R_1^2)}_{\mathcal{R}_1^n} \bar{u}^{(1)} \end{aligned} \quad (87)$$

The restriction operator  $R_{n-1}^n$  thus appears formally as the discrete equivalent of the primary filter  $G_n$ .

Similarly to  $R_n^{n+1}$ , a *Prolongation* operator  $P_{n+1}^n$  is introduced, which allows to perform an interpolation of the variables from the grid level  $\Omega_{n+1}$  to the finest level  $\Omega_n$ . It is to be noted here that such operators do not allow to reconstruct the missing information between the two successive

<sup>1</sup>The two terms *Restriction* and *Prolongation* are commonly used in the multigrid methods terminology.

levels  $n$  and  $n + 1$ . The details (frequency complement) from level  $n$  are then computed as the interpolation error between the two successive levels  $n$  and  $n + 1$  :

$$\begin{aligned}\delta u^{(n)} &= \bar{u}^{(n)} - P_{n+1}^n \bar{u}^{(n+1)} \\ &= (Id - P_{n+1}^n \circ R_n^{n+1}) \bar{u}^{(n)}\end{aligned}\quad (88)$$

Table 2 summarizes the equivalences between the continuous formalism (described in section 3.1) and the discrete formalism considered in the case of a multigrid LES algorithm.

Continuous case	Discrete case
$G_1 \equiv \mathcal{G}_1^1$	$\mathcal{D}_1 : \Omega \rightarrow \Omega_1$
$G_n, n \in [2, N]$	$R_{n-1}^n : \Omega_{n-1} \rightarrow \Omega_n, n \in [2, N]$
$\mathcal{G}_1^n, n \in [2, N]$	$\mathcal{R}_1^n = R_{n-1}^n \circ R_{n-2}^{n-1} \circ \dots \circ R_1^2 : \Omega_1 \rightarrow \Omega_n, n \in [2, N]$

On the basis of such a multilevel decomposition, and to reduce the computational costs associated to LES, Voke proposed to introduce a cycling strategy in time between the different grid levels (the *multiple mesh simulation*), in the restricted case of a two-level flow decomposition. The idea of such an approach is then to reduce the simulation cost by integrating in time on coarse levels, with large time steps, and using finer grids to increase the accuracy of the simulation. A more advanced method, also based on a cycling strategy in time between the different grid levels was then proposed by Terracol and his coworkers. The idea is, at a given time, to perform the simulation only at the most pertinent level. The approach may then be seen as an extended, time-consistent multigrid algorithm. The major hypothesis on which relies the method is that the small scales time variation can be neglected during time integration on coarse resolution levels. This hypothesis is referred to as the *Quasi-Static* (QS) approximation by several authors. Among them, Dubois and his coworkers justified it by exhibiting a very different behavior between the small and the large scales of the flow. In particular, small scales are shown to reach much more quickly a state of equilibrium. Some mathematical estimations of the small scales variation rate were derived, leading to the following result:

$$\left| \frac{\partial}{\partial t} \delta u^{(n)} \right|_2 \ll \left| \frac{\partial}{\partial t} \bar{u}^{(n)} \right|_2 \quad (89)$$

where  $\| \cdot \|_2$  refers to the norm associated to the kinetic energy.

Under this assumption, Terracol *et al.* [43,44] proposed to perform some V-cycles between the different grid levels, in which the solution is advanced successively in time on the different grids. At the end of each cycle, the solution at a given level  $n < N$  is then corrected thanks to the QS approximation:

$$\bar{u}^{(n)} \left( t + \sum_{l=n}^N \Delta t_l \right) = \bar{u}^{(n+1)} \left( t + \sum_{l=n}^N \Delta t_l \right) + \delta u^{(n)}(t) \quad (90)$$

where  $\Delta t_n$  is the integration time at level  $n$ , and the details  $\delta u^{(n)}$  have been kept frozen during time integration on the coarser grid levels. Figure 5 illustrates this algorithm in the restricted case of three filtering levels of the solution.

This algorithm differs from the one proposed by Voke [46] since it incorporates an explicit enrichment procedure of the solution at each grid level at the end of one cycle (by adding the frozen details to the coarser grids solution).

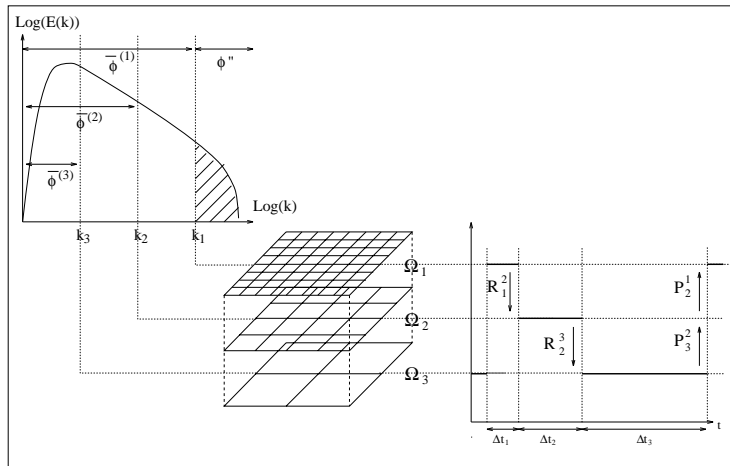


Fig. 5. Schematic representation of the multilevel strategy.

Several aspects of a this multilevel algorithm have been investigated: the first one was dealing with the way to perform the coupling between the different levels. The major point that was pointed out was the problem

of the subgrid closure used on the coarse levels ( $n > 1$ ). It was clearly established that an adapted multilevel subgrid closure (as one of those presented in section 3.3.3) is mandatory on the coarse levels. Indeed, in the case of a more simple coupling between the levels, the results obtained in multilevel simulations were similar to those from a monolevel coarse grid simulation. The second aspect investigated was the way to perform the cycling strategy itself. Indeed, the cycling strategy has to adapt itself dynamically to the unsteadiness of the flow. A dynamic cycling algorithm between the different grid levels was derived, allowing to estimate, at the beginning of each cycle, both the number of grid levels to be considered, and the possible integration time on each level. For this, a criteria, based on a control of the Quasi-Static approximation was introduced. The key idea is then, during one cycle between the grids, to ensure that the time variation of the details at each level remains negligible compared to the time variation of the large scales. In practice such an approach was shown to yield to an effective reduction in CPU time by a factor of up to five (compared to a fine monolevel LES), when three grid levels ( $N = 3$ ) are used [44].

#### 4.1.2. *Partially embedded strategies*

As in the previous section, the idea is here to introduce a hierarchy of embedded grid levels. However, in order to reduce the complexity of the simulation, it appears interesting to adapt this hierarchy of grids in space, in order to use refined grids only in some regions requiring a particular attention. Indeed, classical subgrid closures are generally well-suited for the simulation of flows exhibiting a real large-scale behavior, and in which the effect of the small scales can be represented simply under the classical assumptions of isotropy and homogeneity. The regions of the flow which exhibit such a behavior thus do not require the use of very fine grids. On the other hand such fine grids are mandatory in the regions of the flow in which some small anisotropic and/or inhomogeneous scales are present. In this case, the small scales of the flow cannot be taken into account through the use of a simple subgrid model, and need to be resolved directly (*i.e.* represented by the grid). This is for instance the case in wall-bounded flows, in which the near-wall streaks must be resolved directly.

A simple way to perform such computations, while keeping some affordable CPU requirements, relies on the use of a zonal hierarchy of embedded grids, where the fine grids are only located in some reduced regions of the compu-

tational domain. Obviously, the coarsest grid level  $\Omega_N$  must cover the entire computational domain. Such a configuration is schematically described by figure 6. It appears clearly that such an approach can be seen as a hybrid approach between the zonal and embedded multilevel LES strategies.

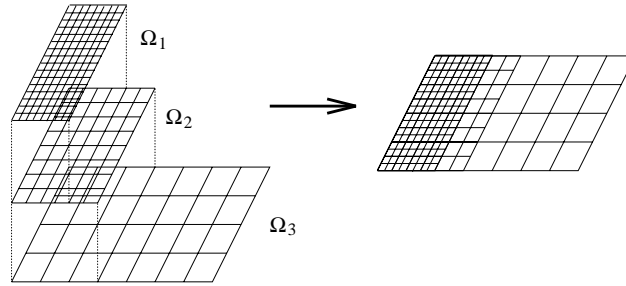


Fig. 6. Zonal multilevel decomposition of a domain  $\Omega$  ( $N = 3$ ).

Such a grid configuration thus allows, as the zonal multilevel methods presented in section 4.2, to get access *locally* to a good accuracy of the simulation (from both the physical and numerical point of views), while keeping some affordable computation costs.

Some specific topological constraints on the grid hierarchy have however to be imposed, in order to guarantee its coherence:

- Two successive grid levels  $n$  and  $n + 1$  ( $n < N$ ) must be properly included:

$$\Omega_n \subset \Omega_{n+1} \quad (91)$$

- The previous inclusion must be strict in the sense that the cells surrounding the grid  $\Omega_n$  must belong to the immediate coarser grid  $\Omega_{n+1}$ , except at the boundaries of the computational domain. Following (91), this is equivalent to the following relation:

$$\Gamma_n \cap \Gamma_{n+1} = \emptyset \quad (92)$$

where  $\Gamma_n$  denotes the boundaries of the grid  $\Omega_n$  which are not some boundaries of the computational domain  $\Omega$ :

$$\Gamma_n = \partial\Omega_n \setminus (\partial\Omega_n \cap \partial\Omega) \quad (93)$$

A simple way to interpret these constraints is just that any grid level  $n$  has only to exchange information with the immediate finer and coarser grid levels  $n - 1$  and  $n + 1$ .

Considering such a zonal multigrid hierarchy, the coupling between the different grid levels is a two-way coupling:

- A coarse-to-fine coupling occurs at the boundaries  $\Gamma_n$  of the fine grid levels ( $n < N$ ) which are not physical boundaries of the domain. At these interfaces, the coupling problem is exactly the same as in the case of the zonal multilevel approach presented in section 4.2. Indeed, at the coupling interface between the level  $n$  and the coarser level  $n + 1$ , it appears *a priori* necessary to take explicitly into account the jump in resolution/representation of the flow variables. For this, an interpolation technique from level  $n + 1$  to level  $n$ , combined with an artificial reconstruction of the missing contribution has to be used.
- A fine-to-coarse coupling occurs from any grid level  $n < N$  to the coarser level  $n + 1$ . In that case, the flow regions resolved at a level  $n$  which are overlapped by a finer grid level  $n - 1$  are reset at each time iteration by interpolating the flow variables from the finer level  $n - 1$  to the grid level  $n$ . This interpolation is carried out by using a restriction operator  $R_{n-1}^n$  such as the ones used in the fully embedded strategies.

It thus appears clearly that partially embedded multilevel strategies appear as some hybrid approaches between fully embedded and zonal multilevel strategies.

**Remark:** A particular case of such a zonal multilevel grid hierarchy can be obtained dynamically thanks to the use of an Adaptive Mesh Refinement (AMR) algorithm. In this case, a refinement sensor has to be defined to detect the regions of the flow where a finer mesh would be required. It should be noted here that there exists a very few works dealing with the problem of deriving such a sensor in the specific context of LES. Indeed, usual sensors are generally based on the local shear of the flow, or on some estimations of the truncation error of the numerical scheme. However some specific sensors should be derived for LES, since the objective should not be here to detect high-shear regions, nor to detect (only) small scales, but to detect the regions of the flow in which the subgrid scales do not satisfy the classical assumptions under which the subgrid models have been developed.

#### 4.2. Zonal multilevel LES

As it has been pointed out in the previous section, an efficient way to reduce the overall cost associated to LES relies on the use of some local mesh refinement strategies. The global idea of these approaches is to use some fine computational grids only in some specific flow regions which require the use of an explicit resolution of the fine flow structures, such as the near-wall region in wall-bounded flows, while using some coarser grids. However, in some other flow regions, where the flow dynamics is simpler to capture. Another practical way to adapt the mesh resolution to the flow physics relies on the use of a multidomain/multiresolution approach in which several computational domains with different mesh sizes are considered. Contrary to what has been presented previously, the different grid levels (domains) do not overlap, *i.e.*  $\Omega_n \cap \Omega_{n+1} = \emptyset$ .

Such strategies raise an important problem since the sudden changes in mesh sizes between adjacent domains are intrinsically linked to some changes in the characteristic sizes of the flow structures. It is to be noted that this problem is generally not accounted for in practical simulations since most of the authors who worked on the subject retained a continuous boundary treatment between the different computational domains. Among others, one can cite the works by Simons *et al.* [38], who retained an approach based on fluxes conservation. A Galerkin method with B-splines basis functions was also developed by Kravchenko *et al.* [24, 23].

However, the use of a continuous treatment of the flow variables at the interface may introduce a buffer region in the fine grid region, in which some smaller scales (unresolved in the coarse grid domain) are progressively regenerated. This may lead to an unexpected behavior of the multidomain simulation when the fine resolution domains have a small extent. Indeed in that case, the buffer region may become as large as the domain, leading to a global coarse grid behavior of the simulation. For that reason, some authors such as Quéméré *et al.* [34] have developed a specific coupling approach between two LES computational domains with different grid resolution. In this approach, the representation discontinuity is explicitly taken into account at the interface between the two domains, leading to a discontinuous treatment for both the flow variables and numerical fluxes. Figures 7 and 8 illustrate the major differences that may occur on the representation of the flow when a continuous and respectively a discontinuous approach is retained for the interface treatment, and more particularly the buffer region

appearing when a continuous treatment is used, and in which small scales are progressively re-generated.

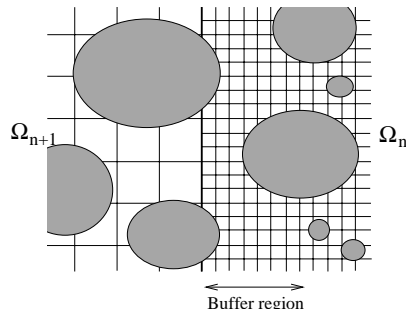


Fig. 7. Zonal multilevel LES with continuous coupling at the interface

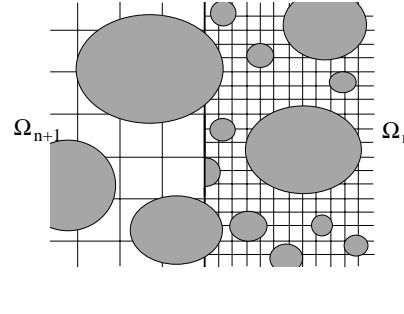


Fig. 8. Zonal multilevel LES with discontinuous coupling at the interface

The discontinuous treatment at the interface proposed by Quéméré *et al.* [34] relies on a two-step strategy:

- (1) The fine-to-coarse coupling from the grid level  $n$  to the grid level  $n + 1$  is relatively easy to perform. A simple restriction operator  $R_n^{n+1}$  such as the ones used for embedded multilevel strategies is applied to the aerodynamic variables resolved at level  $n$ , in order to obtain a value for the filtered field in the ghost cells of the coarser grid level  $n + 1$ . Since such operators act as a low-pass frequency filter on the flow variables, the frequency jump is here explicitly (and in a simple way) taken into account, since it is only required to remove some high-frequency content to the filtered field from level  $n$ .
- (2) The coarse-to-fine coupling from the grid level  $n + 1$  to the grid level  $n$  is somewhat more difficult to perform. As a first step, a classical interpolation operator (prolongation)  $P_{n+1}^n$  is used to obtain some values in the ghost cells of the fine grid domain  $\Omega_n$ . It is to be noted here that this step allows only to provide a field with a frequency content which is equivalent to the one from the coarse grid level  $n + 1$ . Then, in a second step the obtained values have to be modified such that their frequency content matches the one from level  $n$ . For that purpose, the details between the two levels are computed in the fine grid cells adjacent to

the coupling interface, as:

$$\delta u^{(n)} = \bar{u}^{(n)} - P_{n+1}^n \circ R_n^{n+1} \left( \bar{u}^{(n)} \right) \quad (94)$$

In a final step, the values in the ghost cells of the fine grid domain are obtained by adding the details from the last row of the fine grid cells adjacent to the interface to the values in the ghost cells obtained by interpolation from the coarse grid:

$$\bar{u}^{(n)} \Big|_{GC_n} = P_{n+1}^n \left( \bar{u}^{(n+1)} \Big|_{RC_{n+1}} \right) + C_\delta \cdot \delta u^{(n)} \Big|_{RC_n} \quad (95)$$

where  $GC_l$  and  $RC_l$  denote respectively for the grid level  $\Omega_l$  the ghost cells and the real cells close to the interface. The coefficient  $C_\delta$ , referred to as the enrichment constant was introduced by the author to stabilize the simulations. A commonly used value for this coefficient is  $C_\delta \simeq 0.95$ .

The approach was first applied to some plane channel flow computations by Quéméré *et al.* [34]. In these simulations, the approach was used to consider some fine grids in the near-wall region only, while the center part of the channel was computed using a coarser grid domain. Some aspect ratios of up to four between the respective fine and coarse grid cell sizes were considered, together with some different positions of the coupling interface.

This method was also used by some other authors on some more applied configurations. For instance, the computation of the flow over a delta wing was carried out by Mary [31] using this technique, and by Mary and Nolin [32] on a A-airfoil wing profile.

## References

1. J.S. Bagget, J. Jimenez, A.G. Kravchenko. Resolution requirements in large-eddy simulations of shear flows. Annual Research Briefs - Center for Turbulence Research, 51–66, 1997.
2. J. Bardina, J.H. Ferziger, W.C. Reynolds. Improved turbulence models based on large eddy simulation of homogeneous, incompressible, turbulent flows. Report TF-19, Thermosciences Division, Dept. Mechanical Engineering, Stanford University, 1983.
3. L.C. Berselli, T. Iliescu, W.J. Layton. Mathematics of large-eddy simulation of turbulent flows. Springer, Berlin, 2005.
4. D. Carati, M. Rogers, A. Wray. Statistical ensemble of large-eddy simulations. *J. Fluid Mech.* 455: 195–212, 2002.
5. D. Carati, G. Winckelmans, H. Jeanmart. On the modelling of the subgrid-scale and filtered-scale stress tensors in large-eddy simulation. *J. Fluid Mech.* 441, 119–138, 2001.

6. J.A. Domaradzki, N.A. Adams. Direct modelling of subgrid scales of turbulence in large eddy simulations. *JOT* 3(024), 1–19, 2002.
7. J.A. Domaradzki, T. Dubois, and A. Honein. A subgrid-scale estimation model applied to large eddy simulations of compressible turbulence. *Proceedings of the Summer program 1998, Center for Turbulence Research*, pages 351–366, 1998.
8. J.A. Domaradzki and K.C. Loh. The subgrid-scale estimation model in the physical space representation. *Phys. Fluids*, 11(8):2330–2342, 1999.
9. J.A. Domaradzki and P.P. Yee. The subgrid-scale estimation model for high Reynolds number turbulence. *Phys. Fluids*, 12(1):193–196, 2000.
10. T. Dubois and F. Bouchon. Subgrid-scale models based on incremental unknowns for large eddy simulation. *Annual Research Briefs, Center for Turbulence Research*, pages 221–236, 1998.
11. T. Dubois, F. Jauberteau, and R. Temam. Dynamic multilevel methods in turbulence simulation. *Comput. Fluids Dynamics Review*, pages 679–694, 1995.
12. T. Dubois, F. Jauberteau, and R. Temam. A comparative study of multilevel schemes in homogeneous turbulence. In *Lecture Notes in Physics*, volume 490, pages 388–393. Springer Verlag, 1996.
13. T. Dubois, F. Jauberteau, and R. Temam. Incremental unknowns, multilevel methods and the numerical simulation of turbulence. *Comput. Methods Appl. Mech. Engrg.*, 159:123–189, 1998.
14. T. Dubois, F. Jauberteau, and Y. Zhou. Influences of subgrid scale dynamics on resolvable scale statistics in large-eddy simulations. *Physica D*, 100:390–406, 1997.
15. C. Fureby, G. Tabor, G. Mathematical and physical constraints on large-eddy simulations. *Theoret. Comput. Fluid Dynamics* 9: 85–102, 1997.
16. M. Germano, U. Piomelli, P. Moin, and W. H. Cabot. A dynamic subgrid-scale eddy viscosity model. *Phys. Fluids A*, 3:1760–1765, 1991.
17. S. Ghosal, P. Moin. The basic equations for the large-eddy simulation of turbulent flows in complex geometry. *J. Comput. Phys.* 118, 24–37, 1995.
18. T.J.R. Hugues, G.R. Feijóo, L. Mazzei, and J.B. Quincy. The variational multiscale method - a paradigm for computational mechanics. *Comput. Methods Appl. Mech. Engrg.*, 166:3–24, 1998.
19. T.J.R. Hugues, L. Mazzei, and A.A. Oberai. The multiscale formulation of large eddy simulation : Decay of homogeneous isotropic turbulence. *Phys. Fluids*, 12(2):505–512, 2001.
20. T.J.R. Hugues, A.A. Oberai, and L. Mazzei. Large eddy simulation of turbulent channel flows by the variational multiscale method. *Phys. Fluids*, 12(6):1784–1799, 2001.
21. S.A. Jordan. A large-eddy simulation methodology in generalized curvilinear coordinates. *J. Comput. Phys.* 148, 322–340, 1999.
22. B. Knaepen, O. Debligny, D. Carati. Subgrid-scale energy and pseudo pressure in large-eddy simulation. *Phys. Fluids* 14(12), 4235–4241, 2002.
23. A.G. Kravchenko and P. Moin. Numerical studies of flow over a circular cylinder at  $re_d = 3900$ . *Phys. Fluids*, 12(2):403–417, 2000.

24. A.G. Kravchenko, P. Moin, and K. Shariff. B-Spline Method and Zonal Grids for Simulations of Complex Turbulent Flows. *J. Comput. Phys.*, 151:757–789, 1999.
25. E. Labourasse and P. Sagaut. Reconstruction of turbulent fluctuations using a hybrid RANS/LES approach. *J. Comput. Phys.*, 182:301–336, 2002.
26. A. Leonard. Energy cascade in large-eddy simulations of turbulent fluid flows. *Adv. in Geophys. A* 18, 237–248, 1974.
27. M. Lesieur, O. Métais. New trends in large-eddy simulations of turbulence. *Ann. Rev. Fluid Mech.* 28, 45–82, 1996.
28. D.K. Lilly. A proposed modification of the Germano subgrid-scale closure method. *Phys. Fluids A* 4(3), 633–635, 1992.
29. K.C. Loh and J.A. Domaradzki. The subgrid-scale estimation model on nonuniform grids. *Phys. Fluids*, 11(12):3786–3792, 1999.
30. W.D. McComb, A. Hunter, C. Johnston. Conditional mode-elimination and the subgrid-modeling problem for isotropic turbulence. *Phys. Fluids* 13(7), 2030–2044, 2001.
31. I. Mary. Large eddy simulation of vortex breakdown behind a delta wing. *Int. J. Heat and Fluid Flow*, 24:596–605, 2003.
32. I. Mary and G. Nolin. Zonal grid refinement for large eddy simulation of turbulent boundary layers. AIAA paper 2004-0257, 2004.
33. F. Nicoud, F. Ducros. Subgrid stress modeling based on the square of the velocity gradient tensor. *Flow, Turbulence and Combustion* 62(3), 183–200, 1999.
34. P. Quéméré, P. Sagaut, and V. Couaillier. A new multi-domain/multi-resolution method for large-eddy simulation. *Int. J. Numer. Meth. Fluids*, 36:391–416, 2001.
35. P. Sagaut. Large-eddy simulation for incompressible flows, 3rd edition. Springer, Berlin, 2005.
36. P. Sagaut, P. Comte, F. Ducros, F. Filtered subgrid-scale models. *Phys. Fluids* 12(1), 233–236, 2000.
37. U. Schumann. Subgrid scale model for finite difference simulations of turbulent flows in plane channels and annuli. *J. Comput. Phys.* 18, 376–404, 1975.
38. T. A. Simons and H. Pletcher. Large Eddy Simulation of Turbulent Flows Using Unstructured Grids. In *34th AIAA/ASME/SAE/ASEE Joint Propulsion Conference & Exhibit, Cleveland, OH*, July 13–15, 1998.
39. J. Smagorinsky. General circulation experiments with the primitive equations. I: The basic experiment. *Month. Weath. Rev.* 91(3), 99–165, 1963.
40. S. Stolz and N.A. Adams. An approximate deconvolution procedure for large-eddy simulation. *Phys. Fluids*, 11(7):1699–1701, 1999.
41. S. Stolz, N.A. Adams, and L. Kleiser. An approximate deconvolution model for large-eddy simulation with application to incompressible wall-bounded flows. *Phys. Fluids*, 13(4), 2001.
42. S. Stolz, N.A. Adams, and L. Kleiser. An approximate deconvolution model for LES of compressible flows and its application to shock-turbulence interaction. *Phys. Fluids*, 13(10), 2001.

43. M. Terracol, P. Sagaut, and C. Basdevant. A multilevel algorithm for Large Eddy Simulation of turbulent compressible flows. *J. Comput. Phys.*, 167(2):439–474, 2001.
44. M. Terracol, P. Sagaut, and C. Basdevant. A time self-adaptive multilevel algorithm for large-eddy simulation. *J. Comput. Phys.*, 184(2):339–365, 2003.
45. O. Vasilyev, T.S. Lund, P. Moin. A general class of commutative filters for LES in complex geometries. *J. Comput. Phys.* 146, 82–104, 1998.
46. P.R. Voke. Multiple mesh simulation of turbulent flow. Report QMW EP-1082 - University of London, 1990.
47. A. Vreman. The filtering analog of the variational multiscale method in large-eddy simulation. *Phys. Fluids* 15(8), L61–L64, 2003.
48. A. Yoshizawa. A statistically-derived subgrid model for the large-eddy simulation of turbulence. *Phys. Fluids A* 3(8), 2007–2009, 1991.
49. Y. Zang, R.L. Street, and J.R. Koseff. A dynamic mixed subgrid-scale model and its applications to turbulent recirculating flows. *Phys. Fluids A*, 5(12):3186–3196, 1993.